

2025

# Assessing current models of metabolic dysfunction-associated steatotic liver disease: proposing an organoid-based approach for modeling disease progression

---

<https://hdl.handle.net/2144/52266>

*"Downloaded from OpenBU. Boston University's institutional repository."*

BOSTON UNIVERSITY

ARAM V. CHOBANIAN & EDWARD AVEDISIAN SCHOOL OF MEDICINE

Thesis

**ASSESSING CURRENT MODELS OF METABOLIC DYSFUNCTION-  
ASSOCIATED STEATOTIC LIVER DISEASE: PROPOSING AN ORGANOID-  
BASED APPROACH FOR MODELING DISEASE PROGRESSION**

by

**REBECCA FIGUEROA**

B.S., Southern Methodist University, 2023

Submitted in partial fulfillment of the

requirements for the degree of

Master of Science

2025

© 2025 by  
REBECCA FIGUEROA  
All rights reserved

Approved by

First Reader

---

Gwynneth Offner, Ph.D.  
Associate Professor of Medicine

Second Reader

---

Jeannine Foley, Ph.D.  
Assistant Professor of Anatomy and Neurobiology

## **DEDICATION**

I would like to dedicate this work to my mom, Cindy, who has made me the woman I am today and who I would not have gotten this far without. She is strong, she is kind, and she is my everything. Thank you mommy.

## **ACKNOWLEDGMENTS**

I would like to thank Dr. Foley and Dr. Offner for their guidance during the writing process of this thesis. I especially would like to thank Dr. Foley for stepping into the role as my mentor while I was her teaching assistant and for consistently pushing me to reach my full potential. I would also like to thank Brianna Jones and Elijah Nott for being my sounding boards and constantly keeping my head above water during this process.

**ASSESSING CURRENT MODELS OF METABOLIC DYSFUNCTION-  
ASSOCIATED STEATOTIC LIVER DISEASE: PROPOSING AN ORGANOID-  
BASED APPROACH FOR MODELING DISEASE PROGRESSION**

**REBECCA FIGUEROA**

**ABSTRACT**

Metabolic Dysfunction-Associated Steatotic Liver Disease (MASLD) is one of the leading causes of liver disease in the developed world with an ever-increasing prevalence worldwide. There are numerous risk factors associated with the development of MASLD that stem from downstream effects of obesity, adipose tissue dysfunction, excessive lipid delivery to the liver, and more. MASLD exists on a spectrum ranging from hepatic lipid accumulation known as simple steatosis without inflammation to a stage known as Metabolic Dysfunction-Associated Steatohepatitis (MASH) that includes steatosis, inflammation, and varying degrees of fibrosis. This stage, without removal of stressors, has the potential to develop into cirrhosis which may lead to either liver failure or to the development of hepatocellular carcinoma. Although early stages of MASLD are typically asymptomatic, the later stages, including MASH and severe fibrosis, have detrimental effects on liver histology and functionality, eventually leading to mortality. Despite the disease's increasing prevalence and poor outcomes, there are currently no FDA-approved treatment plans for MASLD. The lack of treatment options is due to limitations of existing in vitro and in vivo modeling systems and their inability to faithfully recapitulate MASLD's complexity. This review will investigate the benefits and shortcomings of the various modeling system currently used. In vivo models were

found to stray too far from the genetic profile of humans making it difficult to translate finding associated with treatment methods from these models to humans. It was also discovered that 2D and 3D non-organoid models are limited in their capacity to exhibit late stages of disease progression. The models that most closely resembled the disease characteristics and progression were 3D organoids composed of parenchymal and non-parenchymal liver cell types. A new model was created based on the successes of these 3D organoid models was proposed that has the potential to recapitulate MASLD fully and providing a platform for therapeutic testing.

## TABLE OF CONTENTS

|  |      |
|--|------|
| DEDICATION .....                                   | iv   |
| ACKNOWLEDGMENTS .....                              | v    |
| ABSTRACT.....                                      | vi   |
| TABLE OF CONTENTS.....                             | viii |
| LIST OF TABLES .....                               | x    |
| LIST OF FIGURES .....                              | xi   |
| LIST OF ABBREVIATIONS.....                         | xii  |
| BACKGROUND .....                                   | 1    |
| Overview of MASLD .....                            | 1    |
| Liver Overview and Fatty Acid Metabolism .....     | 2    |
| Regeneration and its Boundaries .....              | 8    |
| What is MASLD? .....                               | 9    |
| Risk Factors for MASLD.....                        | 11   |
| Pathogenesis and Pathophysiological of MASLD ..... | 18   |
| Diagnosis and Stages of MASLD.....                 | 28   |
| Management and Treatment Options.....              | 31   |
| SPECIFIC AIM.....                                  | 35   |
| EVALUATING THE MODELING TECHNIQUES FOR MASLD.....  | 36   |
| DISCUSSION .....                                   | 65   |
| CONCLUSION.....                                    | 74   |
| BIBLIOGRAPHY.....                                  | 75   |

VITA..... 85

## LIST OF TABLES

|   |    |
|---|----|
| Table 1: Genes associated with MASLD development and progression..... | 15 |
|---|----|

## LIST OF FIGURES

|  |    |
|--|----|
| Figure 1: Schematic of hepatocyte polarity .....   | 4  |
| Figure 2: Fatty acid oxidation and fatty acid synthesis main steps.....  | 7  |
| Figure 3: MASLD Spectrum and factors associated with progression.....  | 10 |
| Figure 4: The factors involved in hepatic fat accumulation .....   | 21 |
| Figure 5: OS Liver Injury in MASH.....   | 25 |
| Figure 6: Progression from MASH to fibrosis.....   | 28 |
| Figure 7: Balance between oxidants and anti-oxidants.....  | 33 |
| Figure 8: Characteristics of MASLD exhibited after FA exposure to HML organoids. ..  | 39 |
| Figure 9: Depicting types of liver organoids .....   | 46 |
| Figure 10: Profibrotic and proinflammatory makers induced in 3D-hLMTs after PA<br>treatment .....                            | 49 |
| Figure 11: The process of forming 3D liver organoids on a chip through hiPSC<br>differentiation.....                         | 56 |
| Figure 12: H&E staining of SC, FF, and HF diet fed mice on the left and Masson's<br>Trichrome of each diet on the right..... | 61 |
| Figure 13: MASH-treated hLiMTs exhibited steatosis-like phenotype and lipid<br>accumulation .....                            | 64 |

## LIST OF ABBREVIATIONS

|               |   |
|---------------|---|
| 3D-hLMT ..... | Three-Dimensional Human Liver Microtissue                         |
| Akt.....      | Protein Kinase B  |
| ALT.....      | Alanine Aminotransferase  |
| AST .....     | Aspartate Aminotransferase  |
| AT .....      | Adipose Tissue  |
| BSA.....      | Bovine Serum Albumin  |
| BSEP .....    | Bile Salt Export Pump   |
| CDAHFD .....  | Choline-Deficient, Amino Acid-Defined High-Fat Diet               |
| CDAHFD-F..... | Choline-Deficient, Amino Acid-Defined High-Fat Diet with Fructose |
| CDAHFD-S..... | Choline-Deficient, Amino Acid-Defined High-Fat Diet with Sucrose  |
| COs .....     | Cholangiocyte Organoids   |
| DAMPs .....   | Damage-associated molecular patterns                              |
| DNL .....     | De novo Lipogenesis   |
| ECM.....      | Extracellular Matrix  |
| ETC .....     | Electron Transport Chain  |
| FAS .....     | Fatty Acid Synthase   |
| FBS .....     | Fetal Bovine Serum  |
| FF .....      | Fast food   |
| FFAs.....     | Free Fatty Acids  |
| FFC .....     | High fat, fructose, and cholesterol Diet                          |
| GLP-1 .....   | Glucagon-like Peptide-1 Receptor                                  |

|                      |  |
|----------------------|--|
| H&E .....            | Hematoxylin and Eosin                                    |
| HCC .....            | Hepatocellular Carcinoma                                 |
| HES .....            | Heamalin-Eosin-Saffron Reagent                           |
| HF .....             | High-Fat   |
| hiPSC .....          | Human-Induced Pluripotent Stem Cell                      |
| hLiMTs .....         | Human Liver Microtissues                                 |
| HNF-4 $\alpha$ ..... | Hepatocyte Nuclear Factor-4 alpha                        |
| HOs .....            | Hepatocyte organoids COs                                 |
| hPSCs .....          | Human Pluripotent Stem Cells                             |
| HSCs .....           | Hepatic Stellate Cells                                   |
| ICOs .....           | Intrahepatic Cholangiocyte Organoids                     |
| IGFBP2 .....         | Insulin-like Growth Factor-Binding Protein-2             |
| IL-1 $\beta$ .....   | Interleukin-1 $\beta$                                    |
| IR .....             | Insulin Resistance                                       |
| IRS .....            | Insulin Receptor Substrate                               |
| KCs .....            | Kupffer Cells  |
| LECs .....           | Liver Endothelial Cells                                  |
| LPS .....            | Lipopolysaccharide                                       |
| LXRs .....           | Liver X Receptors  |
| MASLD .....          | Metabolic Dysfunction-Associated Steatotic Liver Disease |
| MASH .....           | Metabolic Dysfunction-Associated Steatohepatitis         |
| MCD .....            | Methionine- and Choline-Deficient                        |

|                      |  |
|----------------------|--|
| MS.....              | Metabolic Syndrome                               |
| NAFLD.....           | Non-Alcoholic Fatty Liver Disease                |
| NAS.....             | NAFLD Activity Score                             |
| NASH.....            | Non-Alcoholic Steatohepatitis                    |
| NEFAs.....           | Non-esterified Fatty Acids                       |
| OA.....              | Oleic Acid                                       |
| OS.....              | Oxidative Stress                                 |
| PA.....              | Palmitic Acid                                    |
| PFA.....             | Paraformaldehyde                                 |
| PI3K.....            | Phosphatidylinositol-3 Kinase                    |
| PPAR- $\alpha$ ..... | Peroxisome Proliferator-activated Receptor alpha |
| ROS.....             | Reactive Oxygen Species                          |
| RT-PCR.....          | Real-time PCR                                    |
| SREBPs.....          | Sterol Regulatory Element Binding Proteins       |
| T2DM.....            | Type 2 Diabetes-Mellitus                         |
| TCA.....             | Tricarboxylic Acid Cycle                         |
| TGs.....             | Triglycerides                                    |
| TNF- $\alpha$ .....  | Tumor Necrosis Factor- $\alpha$                  |
| TSP1.....            | Thrombospondin 1                                 |
| VLDL.....            | Very Low-Density Lipoprotein                     |

## **BACKGROUND**

### **Overview of MASLD**

Metabolic dysfunction-associated steatotic liver disease (MASLD) is one of the primary drivers in chronic liver disease in the western world (Pouwels et al., 2022). In 2018, it was estimated that the global prevalence of MASLD was 25% (Gerges et al., 2021) and that number was estimated to have increased by 10% in 2023 (Wong et al., 2023). Its prevalence is continuously growing concurrently with the spread of obesity and Type 2 Diabetes-Mellitus (T2DM) (Gerges et al., 2021) as these are some of the most common comorbidities seen in MASLD. This disease is thought to be the hepatic manifestation of metabolic syndrome (MS) (Carr et al., 2016). Metabolic syndrome is the grouping of increased waist circumference (central obesity), hyperglycemia, dyslipidemia, and systemic hypertension (Huang, 2009). MASLD is also associated with similar metabolic disorders including dyslipidemia, central obesity, hyperglycemia, and hypertension (Pouwels et al., 2022). It is considered the hepatic manifestation of MS because it incorporates a range of liver conditions from simple fat accumulation, known as steatosis, to metabolic dysfunction-associated steatohepatitis (MASH), fibrosis, cirrhosis, and hepatocellular carcinoma. It is also known as a chief cause of end-stage liver disease and liver transplantation (Powell et al., 2021).

MASLD was once known as Non-Alcoholic Fatty Liver Disease (NAFLD) and MASH was known as Non-Alcoholic Steatohepatitis (NASH). The original term NASH, was chosen in 1980 because of the disease's close resemblance to alcohol-associated liver disease but in patients who do not consume alcohol. With advances in the scientific

field's understanding about the disease it became clear that it must be renamed. The disease is associated with underlying insulin resistance, adipose tissue dysfunction, and has a rather heterogenous profile. The new terms, MASLD and MASH more accurately reflect the nature and pathogenesis of this disease (Rinella & Sookoian, 2023). Although the scientific papers cited by this thesis use the old terms NAFLD and NASH, this thesis will use the new, more accurate terms of MASLD and MASH.

### **Liver Overview and Fatty Acid Metabolism**

The liver is an organ responsible for numerous vital processes in the body. These include metabolism, digestion, detoxification, immunity, and vitamin storage. It develops from the foregut through complex signaling pathways like MAPK induction of fibroblast growth factor release and Wnt- $\beta$ -catenin pathways. These signals cause the hepatic cords to form around the portal vein allotting it to become the central vessel and main blood supply (Kalra et al., 2025). This unique blood supply, where the liver receives most of its blood flow from the portal vein and the rest from the hepatic artery, allows it to participate in its many functions (Kalra et al., 2025). The portal vein is responsible for delivering blood from the gastrointestinal tract to the liver thus creating an important gut-liver axis that has numerous disease implications (Gerges et al., 2021).

The liver is composed of parenchymal and non-parenchymal cells. The parenchyma, or functional portion, of the liver is composed of liver cells, known as hepatocytes, that are arranged into lobules. Each lobule has a portal triad at the corner of their roughly hexagonal shape that is composed of portal vein, hepatic artery, and a bile duct. The hepatocytes are further divided into three zones that differ in their perfusion

and function. Zone 1 is well-perfused and plays a role in oxidative metabolism and zone 2 is the least perfused but plays a role in detoxification, glycolysis, lipogenesis, ketogenesis, glycogen synthesis, and glutamine formation (Kalra et al., 2025). The liver also contains bile ducts which are lined by epithelial cells called cholangiocytes (Han et al., 2023). These cells function to produce, modify, and detoxify bile (Ehrlich et al., 2018). Bile production is important for the liver as it aids in lipid digestion and absorption as well as waste excretion, such as cholesterol (Kalra et al., 2025).

Hepatocytes are polarized, meaning they have distinct apical and basal membranes that are physiologically responsible for different processes, shown in Figure 1. The basolateral membrane forms a space with the sinusoidal lumen known as the space of Disse. The space of Disse is composed of materials such as proteoglycans, scaffolding proteins, and collagen that allow it to provide a scaffolding for the hepatocyte and liver lobules. Contained in this space are various non-parenchymal cells of the liver such as Kupffer cells and Hepatic Stellate Cells (HSCs) (Kalra et al., 2025). The liver contains two macrophage populations, monocyte-derived ones, and Kupffer cells, which are the resident macrophages. Kupffer cells account for 90% of the macrophage population and play a role in regulating and maintaining immunity. These cells and their chemokines and cytokines participate in crosstalk that activates HSCs. HSCs account for 5-8% of all liver cells and serves to store Vitamin A in lipid droplets. They are typically quiescent but upon activation they transdifferentiate into myofibroblasts that deposit additional extracellular matrix (ECM) molecules. Activated HSCs are capable of proliferating, migrating, contracting, and becoming fibrogenic (Han et al., 2023).

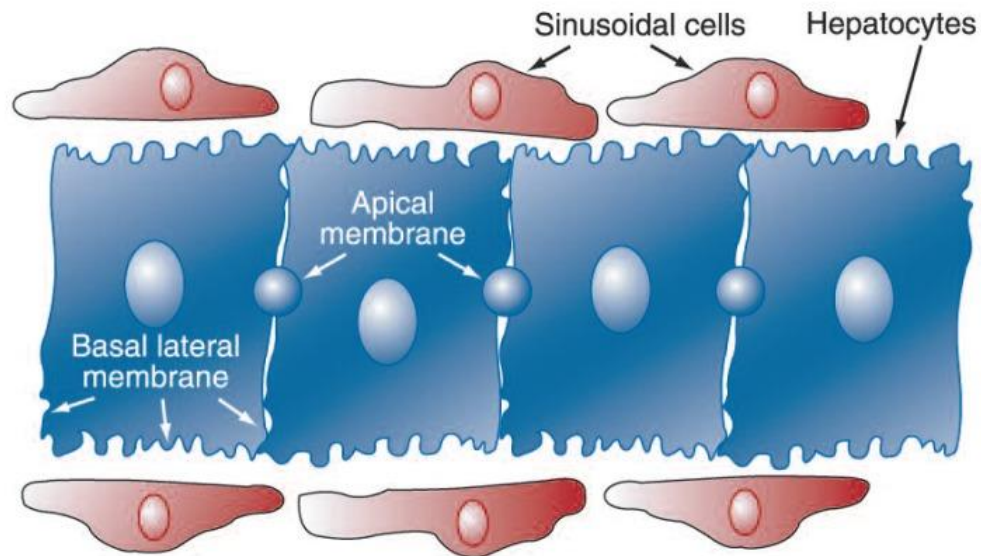


**Figure 1:** Schematic of hepatocyte polarity (Clemens, 2006)

As mentioned, the liver plays an important role in lipid metabolism, especially with fatty acids as they are the most predominant stored and circulating form of energy. The major non-toxic form of fatty acids are triacylglycerols. There are four inputs of the fatty acids that are of note: 1) adipose tissue lipolysis gives rise to plasma non-esterified fatty acids, 2) cytoplasmic triacylglycerol stores, 3) De novo lipogenesis, and 4) fatty acids from triacylglycerols of lipoprotein remnants that were taken up by the liver. Although there are four inputs, there are only two outputs: 1) constituents of very low-density lipoprotein (VLDL) that are secreted by the liver or 2) accumulating in hepatocytes. Since there are a limited number of outputs the liver is rather susceptible to lipid overload that results in fatty acids accumulating in the cells. Cellular molecules act as triacylglycerol content regulators within hepatocytes and influence fatty acid uptake, synthesis, esterification, and oxidation as well as triacylglycerol export (Nguyen et al., 2008).

The liver takes up non-esterified fatty acids (NEFAs) through diffusion or through transporters along the hepatocyte cell membrane. These NEFAs can arise through the breakdown of complex lipids via lipase or of fatty acid-CoA via thioesterases. Once in the hepatocyte, fatty acids undergo covalent binding and activation mediated by fatty acid binding protein or acyl-CoA synthetase and transported intracellularly for metabolism or transcription factor interaction in the nucleus. Fatty acids from outside of the body are rapidly neutralized, polarized, or oxidized. All these steps are taken to ensure intracellular fatty acyl-CoA and NEFA levels remain very low (Nguyen et al., 2008).

The liver can perform de novo synthesis of fatty acids, also known as de novo lipogenesis (DNL), where it creates fatty acids from other biological molecules. The fatty acids made during this process are exported as lipoproteins and used as an energy source (Nguyen et al., 2008). This process is enhanced by a high carb, low fat diet, hyperinsulinemia and inhibited by fasting or a high fat diet (Koek et al., 2011; Nguyen et al., 2008). There is a tight regulation between insulin concentration and DNL through the enzyme fatty acid synthase (FAS). FAS is responsible for catalyzing the pathway of palmitate synthesis, the primary product of DNL. Insulin activates this pathway while glucagon, the stored form of glucose, and catecholamines inhibit it (Nguyen et al., 2008). This regulation becomes increasingly important when there is a dysregulation of insulin secretion or sensitivity which will be discussed later. DNL is Sterol regulatory element binding proteins (SREBPs) and this regulation is mediated by nuclear liver X receptors (LXRs) and transcription factors such as Sterol regulatory element binding proteins (SREBPs). Insulin expression causes a rise in SREBP expression while glucagon and

cAMP leads to a decrease. Over-expression of SREBP-1a increases FAS activity eventually leading to triglyceride (TG) accumulation if not restricted (Nguyen et al., 2008).

Short, medium, and long chain activated fatty acids or non-esterified acyl-CoAs are broken down via oxidation by mitochondria or peroxisomes, shown in Figure 2. Within the mitochondria, fatty acyl-CoA is subjected to  $\beta$ -oxidation becoming acetyl-CoA which is then further oxidized to CO<sub>2</sub> in the tricarboxylic acid cycle (TCA). An enzyme along the outer mitochondrial membrane, CPT-I regulates the entry of long-chain fatty acids into the mitochondria. It catalyzes the formation of acyl-carnitine from fatty acid acyl groups which is then transported by a carrier across the mitochondrial membrane. CPT-II converts acyl-carnitine back to acyl-CoA once it is inside the mitochondria. This process is inhibited by malonyl-CoA, a product of the first step of DNL. If there is a negative energy balance in the body malonyl-CoA content decreases which decreases CPT-I inhibition and therefore increases fatty acid oxidation. Without this negative energy balance or with an abundance of DNL stimulators,  $\beta$ -oxidation is inhibited, and the liver is at risk of accumulating FAs in the form of TGs. While mitochondria take care of much of the FAs, peroxisomes are responsible for breaking down very long-chain FAs. These FAs are metabolized by cytochrome P450 CYP4A via  $\omega$ -oxidation into dicarboxylic acids. The peroxisomal pathway also acts as a spillover pathway to handle the surplus of fatty acids in an attempt to maintain lipid homeostasis. If both pathways, mitochondrial and peroxisomal are overwhelmed then lipid homeostasis is at risk and accumulation within the cells can occur (Nguyen et al., 2008).

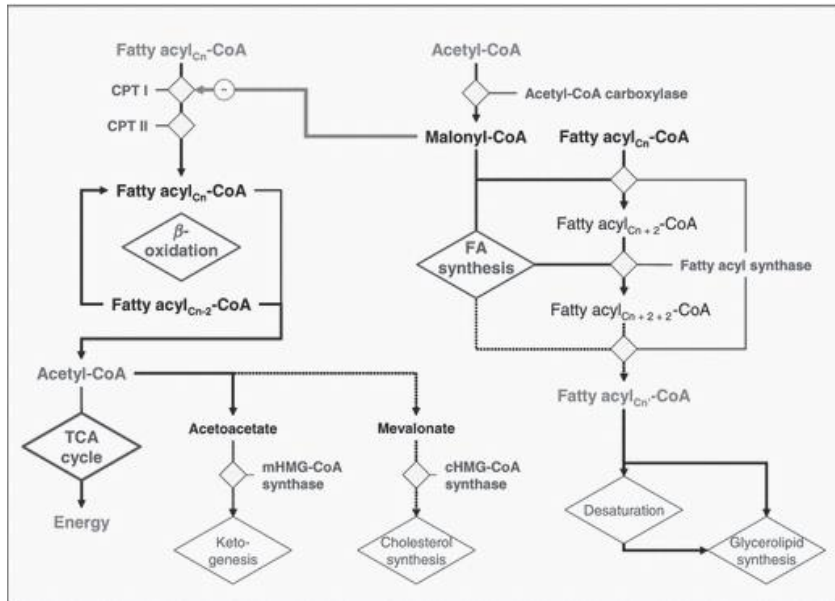


**Figure 2:** Fatty acid oxidation and fatty acid synthesis main steps (Nguyen et al., 2008)

Triacylglycerols are exported from the tissue through VLDL synthesis and secretion (Nguyen et al., 2008). Free fatty acids (FFAs) from dietary TGs are metabolized in the liver, adipose tissue, and muscle. They are then re-esterified to TGs in the liver and excreted into the circulation as VLDL. These VLDLs and circulating chylomicrons then attach to lipoprotein lipase on the endothelial lining of capillaries which allows FFAs to be released (Koek et al., 2011). The rate of synthesis of a particular protein, Apoprotein B100, in the rough endoplasmic reticulum control the total production rate for VLDL. Apoprotein B receives lipids synthesized in the smooth endoplasmic reticulum from microsomal triacylglycerol transfer protein. Once carried into the Golgi apparatus, the apoproteins are glycosylated and then vesicles bud off carrying the apoproteins, move to the sinusoidal membrane where they fuse and release VLDL into the blood. Fatty acid availability may not be the only determinate of the rate of VLDL production; rather the source of fatty acids integrated into TGs can affect the rate of VLDL export. For

example, it was reported that in obese mice DNL did not stimulate VLDL output. It was found that plasma NEFA has a role in enhancing hepatic esterification and stimulating VLDL production (Nguyen et al., 2008).

As briefly mentioned, insulin plays an important role in fat, protein, and carbohydrate metabolism (Koek et al., 2011). Under normal conditions, insulin promotes glucose to be taken up by the skeletal muscle and the liver. Once taken up, the glucose can either be oxidized and used as a fuel or stored as glycogen (Gerges et al., 2021). In adipose tissue (AT), insulin promotes the synthesis of TGs and inhibits lipolysis which is the breakdown of lipids. In the liver, this hormone suppresses glucose production and stimulates DNL to synthesize TGs. Insulin functions through binding to a specific receptor that upon binding undergoes tyrosine phosphorylation which activates downstream targets such as Insulin Receptor Substrate (IRS), Phosphatidylinositol-3 Kinase (PI3K), and Protein Kinase B (Akt). Akt, specifically, mediates insulin acting on glucose and lipid metabolism as well as inhibiting gluconeogenesis. Insulin resistance (IR), briefly, is when even though insulin levels are normal or possibly elevated, there is a diminished cellular response to insulin-driven glucose uptake (Koek et al., 2011). This resistance and its implications in disease development and progression will be discussed later.

### **Regeneration and its Boundaries**

The liver is unique in that it possesses the capability to regenerate upon damage. Liver regeneration is a three-phase process: 1) initiation – hepatocyte activation, 2) proliferation – cell division, and 3) termination, which is regulated by inhibitory

molecules. This process also involves numerous pathways such as activation of liver progenitor cells, immune cell recruitment, and extracellular matrix remodeling. Liver regeneration, however, is limited depending on the type of injury and the extent of the injury. Upon acute liver injury, the liver can regenerate efficiently. But upon chronic liver injury or disease, the capacity of the hepatocytes to regenerate may be exhausted. Liver injury triggers the immune system to release cytokines such as Tumor Necrosis Factor- $\alpha$  (TNF-  $\alpha$ ) and Interleukin-1 $\beta$  (IL-1 $\beta$ ), which either encourage regeneration or contribute to fibrosis. If the inflammation is persistent and chronic, regeneration may be impaired, and the tissue can eventually become cirrhotic. For example, viral infection, metabolic dysfunction-associated steatohepatitis (MASH), alcoholic liver disease, and drug-induced liver injury, can lead to irreversible damage by inducing prolonged lipotoxicity, oxidative stress, and inflammation that cause fibrosis and cirrhosis to develop (Hora & Wuestefeld, 2023; Koek et al., 2011).

### **What is MASLD?**

MASLD is a chronic liver disease characterized by hepatic accumulation of lipids, specifically TGs, known as steatosis, in more than 5% of hepatocytes (Juanola et al., 2021). Some call MASLD a disease of exclusion because it occurs in the absence of alcohol consumption (<20 grams of ethanol/day), drug use, and viral induce steatosis (Juanola et al., 2021; Pouwels et al., 2022). MASLD exists on a spectrum, shown in Figure 3, from simple steatosis to metabolic dysfunction-associated steatohepatitis (MASH), and ultimately fibrosis, cirrhosis, and liver failure or possibly hepatocellular carcinoma (HCC). Steatosis, as mentioned, is the accumulation of hepatic triglycerides,

with or without inflammation or fibrosis. Steatosis is typically asymptomatic aside from elevated liver enzymes, that is until it progresses to MASH in approximately 20-30% of patients. If symptoms are present, they are mild such as fatigue, right upper quadrant pain and hepatomegaly (enlarged liver) on physical examination. MASH consists of steatosis with lobular inflammation, hepatocellular injury seen as ballooning, and apoptosis. Of patients that progress to MASH approximately 41% progress to fibrosis and 25% progress to cirrhosis. MASLD patients may exhibit one or more features of metabolic syndrome which includes but is not limited to insulin resistance, dyslipidemia, system hypertension, and overt diabetes (Delli Bovi et al., 2021; Gerges et al., 2021; McCullough, 2006; Pouwels et al., 2022).

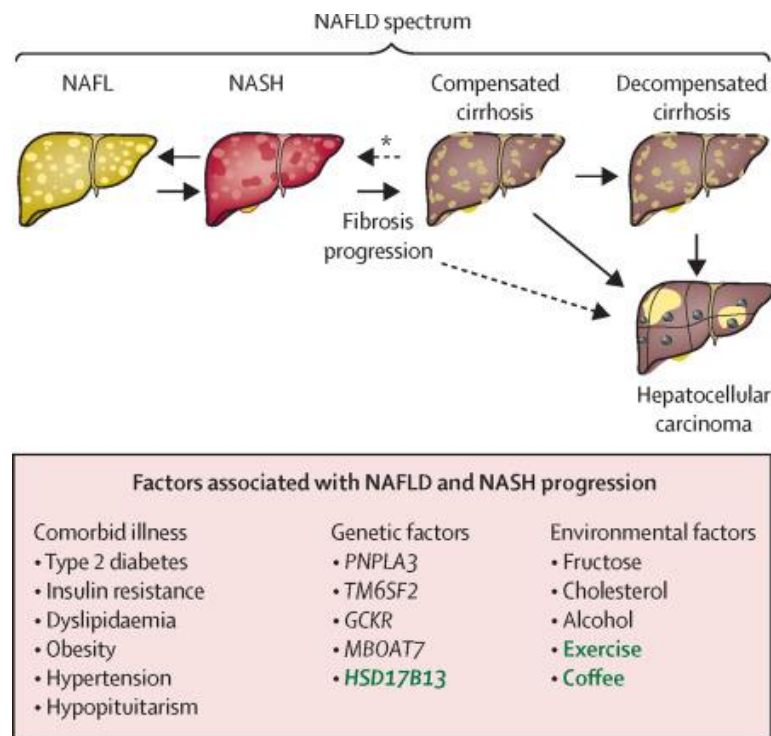


**Figure 3:** MASLD Spectrum and factors associated with progression (Powell et al., 2021)

### **Risk Factors for MASLD**

MASLD has a large and wide list of risk factors that include metabolic risk factors such as obesity, metabolic syndrome, and insulin resistance; genetic factors; epigenetic factors such as DNA methylation and miRNAs; demographic factors such as age, gender and ethnicity; and environmental risk factors such as air pollution, toxins, and diet and lifestyle. Of the metabolic risk factors, obesity is a main risk for MASLD (Juanola et al., 2021).

Numerous studies reported that in obese patients receiving bariatric surgery there was an MASLD prevalence of 57-91% (Masuoka & Chalasani, 2013). Obese patients tend to have lipotoxic and glucotoxic physiological environments that promote steatosis and progression to MASH. These patients typically consume high fat and carbohydrate diets that lead to fat deposition in the liver via ER and oxidative stress and mitochondrial defects. Without management of these stressors, inflammation occurs where innate immune cells are activated and infiltrate the liver release cytokines that lead to added inflammation and eventually fibrogenesis. Obesity also leads to the release of adipokines and hormones that further progress the disease (Juanola et al., 2021). A study that investigated childhood adiposity and MASLD in adulthood found that obese children were more likely to develop MASLD as adults than children of normal weight. It was also found that regardless of childhood weight status, obese adults were at a greater risk of developing MASLD than non-obese adults (Yan et al., 2017).

Obesity is a primary risk factor of MASLD and evidence from various studies prove this by showing loss of weight can reverse MASLD features and risk (Bence &

Birnbaum, 2021). As concluded by the Meta-Analysis conducted by Mummadi et al., weight loss through bariatric surgery was successful at improving 90% of steatosis and 80% of MASH features in patients (Mummadi et al., 2008). The use of glucagon-like peptide-1 receptor (GLP-1) agonists to treat MASH was successful as their true targets are obesity and T2DM. 59% of patients that received a 0.4 mg daily dose of the GLP-1 agonist, semaglutide, subcutaneously experience MASH resolution, which was 42% higher than the placebo (Newsome et al., 2021).

Another metabolic risk factor is metabolic syndrome (MS) which was briefly discussed previously and defined as an increased waist circumference and having hyperglycemia, dyslipidemia, systemic hypertension, obesity, and T2DM (Gerges et al., 2021; Juanola et al., 2021). MASLD prevalence is elevated among MS patients since it is the hepatic component of MS (Gerges et al., 2021). There is a bidirectional association between MS and MASLD risk where having MS increased the risk of obtaining MASLD whereas treatment of MASLD could improve MS features. In patients with MS, insulin's capacity to inhibit glucose production is decreased which leads to hyperglycemia. Hyperglycemia then leads to more insulin released and eventually hyperinsulinemia. This dysfunctional insulin relationship causes it to be unable to suppress the synthesis of TG-rich VLDL particles or lipolysis which leads to an increase in serum TGs further exasperated liver lipid overload in MS and MASLD patients. As a result of this dyslipidemia, there is a decrease in HDL cholesterol and increase in LDL production both of which are highly atherogenic, greatly increasing the potential of developing cardiovascular disease (Juanola et al., 2021). MASH development is also more common

and progression to fibrosis and cirrhosis and more likely in MASLD patients with MS (Gerges et al., 2021).

Diabetes and insulin resistance are also risk factors of MASLD and very common comorbidities. As mentioned, insulin resistance is when there is a diminished cellular response to insulin-driven glucose uptake even when insulin levels are normal or increased. Systemic insulin resistance causes the pancreas to release more insulin in order to regulate peripheral glucose uptake issues and suppresses liver glucose production. This pancreatic insulin is transported to the liver via the portal vein where normally it stimulates glycogenesis, inhibits gluconeogenesis, and activates DNL. It also acts on adipose tissue to increase lipogenesis by esterifying FAs and inhibits lipolysis (Gerges et al., 2021). With insulin resistance, the opposite of these processes occurs leading to an increase in free fatty acid delivery to the liver which can induce steatosis. The presence of these two diseases in a patient act as a determinant for MASLD progression to MASH, fibrosis, and eventually HCC development (Juanola et al., 2021). T2DM specifically doubles the risk that a patient develops advanced fibrosis, cirrhosis-related complications, or liver disease mortality (Powell et al., 2021).

The gut microbiome is composed of 10-100 trillion microorganisms that are susceptible to pathophysiological and environmental alterations. The human gut microbiome affects hepatic lipid and carbohydrate metabolites as well as influences the balance between pro- and anti-inflammatory effectors. These factors have direct effects on MASLD and its progression to MASH. It is, however, unclear whether it is the poor dietary habits seen in obese patients that lead to MASLD or the microbiome disruption

itself (Juanola et al., 2021). A study conducted by Roy et al., established that the transfer of a microbiome from mice with hyperglycemia and insulinemia into germ free mice led to the development of MASLD in recipient mice. This is of note since the transfer of the microbiome from healthy mice did not elicit the same response (Roy et al., 2013).

Another piece of evidence that shows microbiome alterations may contribute to MASLD development and progression is the finding of bacterial species known to be associated with MASLD in abundance in MASH patients compared to healthy individuals. It was also found that there was an increase in specific phylum of these two bacteria during MASLD progression indicating that the microbiome undergoes fluctuations during the progression of this disease (Boursier et al., 2016; Loomba et al., 2017; Zhu et al., 2013). Further support for the microbiome contribution to MASLD pathogenesis is found in a study that treated MASLD patients with the antibiotic rifaximin. Rifaximin targets gram-negative bacteria and therefore inhibits endotoxin proinflammatory cytokine production in these patients. It was found to successfully and robustly reduce endotoxin and IL-10 levels as well as improve steatosis and MASH (Gangarapu et al., 2015).

There are certain genetic factors that leave patients at risk for MASLD development such as heritability and gene loci that play a role in lipid metabolism within hepatocytes. Immediate family members are at a greater risk for MASLD and therefore have a genetic predisposition. If a patient has a parental history of the disease they are at risk even if they themselves are healthy. Certain studies found that heritability of steatosis, fibrosis, and serum alanine aminotransferase (ALT) levels was greater in monozygotic twins than dizygotic twins. This typically supports that there is a genotype

relevance to the heritability. Gene loci that are implicated in the heritability of MASLD include PNPLA3, TM6SF2, GCKR, MBOAT7, and HSD17B14 (Juanola et al., 2021).

Table 1 goes into more detail about these loci and the epigenetic signatures discussed below.

**Table 1:** Genes associated with MASLD development and progression (Juanola et al., 2021)

| Gene                           | Tissue Expression                         | Function  | Main Alterations/Variants   | Effect  |
|--------------------------------|---|---|---|---|
| <i>PNPLA3</i>                  | Liver, adipose tissue and retina          | Lipid droplet remodeling, Lipid metabolism [87,88]                                | Loss of function mutations: rs738409 C>G/p.1148M [83]   | ↑ NAFLD, NASH, fibrosis, HCC [89,90,91,92,93]                         |
| <i>TM6SF2</i>                  | Liver and small intestine                 | VLDL and cholesterol trafficking and secretion [94,95]                            | Loss of function mutations: rs58542926 C>T/p.E167K [96]   | ↑ NAFLD, NASH, fibrosis [97,98,99,100]                                |
| <i>GCKR</i>                    | Mainly liver                              | Regulation <i>de novo</i> lipogenesis, Blood glucose homeostasis [101]            | Loss of function mutations: rs1260326 C>T/p.P446L and rs780094 C>T/intronic [102]                     | ↑ NAFLD, NASH, fibrosis [102,103,104,105]                             |
| <i>MBOAT7</i>                  | Ubiquitous, Liver enriched                | Phosphatidylinositol remodeling [106]   | Loss of function mutations: rs641738 (C>T)? [107]   | ↑ NAFLD, NASH, fibrosis [108,109]                                     |
| <i>HSD17B13</i>                | Ubiquitous, Liver enriched                | Lipid droplet remodeling, Retinol metabolism [110]                                | Loss of function mutations: rs72613567 A>T/intronic and rs143404524/frame shift [111,112,113,114,115] | Protective effect, ↓ NAFLD, NASH, fibrosis, HCC [111,112,113,114,115] |
| <i>IGFBP2</i>                  | Mainly liver and kidney                   | IGF factors transportation [116]  | Hypermethylation, Reduced expression, [116]   | ↑ NAFLD [116]   |
| <i>PGC1<math>\alpha</math></i> | Muscles, liver, adipose tissue and kidney | Energy metabolism and mitochondrial biogenesis [117]                              | Hypermethylation, Histone hypoacetylation, Reduced expression [117]                                   | ↑ NAFLD, NASH [117]   |
| <i>SIRT1</i>                   | Ubiquitous                                | Histone deacetylase, Regulates several genes involved in metabolism control [118] | Reduced expression [119]  | ↑ NAFLD [119,120]   |
| <i>miR-122</i>                 | Ubiquitous, Liver enriched                | Regulation of lipid metabolism and fibrogenesis [121,122,123]                     | Reduced expression in the liver [124]   | ↑ NAFLD, NASH, fibrosis, HCC [125,126]                                |
| <i>miR-34</i>                  | Ubiquitous                                | Regulates lipophagy, Negatively regulates <i>SIRT1</i> [127,128]                  | Liver overexpression [127,128]  | ↑ NAFLD [127,128]   |

Epigenetics describes heritable yet reversible changes in gene expression that occur without alterations to the DNA sequence itself and is associated MASLD risk. There have been epigenetic modifications found in embryo development associated with maternal obesity, diabetes, and a Western diet consumption that contributed to a harsh intrauterine environment. This unfavorable environment induces liver mitochondrial dysfunction that leads to damage and metabolic reprogramming within the embryo that leaves them with a lifetime risk of MASLD. DNA methylation is a process that leads to epigenetic modifications. Hypomethylation is associated with MASLD and is seen to correlate with the severity of disease (Juanola et al., 2021). Specific fibrogenesis genes were hypomethylated and therefore upregulated such as TGF- $\beta$ , Collagen 1A1, and

platelet-derived growth factor (Zeybel et al., 2015). Hypermethylated and therefore reduced expression was seen in insulin-like growth factor-binding protein-2 (IGFBP2). This preceded the development of steatosis when mice were metabolically stable (Kammel et al., 2016). Since IGFBP2 expression was shown to be reduced prior to steatosis development, it may be a potential risk indicator of NALFD development. miRNAs are another epigenetic example that are responsible for regulating lipid uptake, DNL, lipid oxidation, apoptosis, cell proliferation, hepatic lipid export, and fibrosis (Juanola et al., 2021). miR-33a and miR-33b regulate ATP-binding cassette transporter 1 levels negatively, which are an HDL biogenesis control. This promotes high levels of VLDL and TGs which can lead to the development of MASLD (Horie et al., 2010). miR-34 is identified as being overexpressed in MASLD. This micro-RNA represses lipophagy by reducing mitochondrial oxidation and eventually leading to lipid accumulation in the liver (Juanola et al., 2021). All of these epigenetic modifications may individually or together leave a patient at risk of developing MASLD or for the disease to progress.

Demographic factors such as age, gender, ethnicity, and race have strong implication in MASLD development. There is a strong correlation between age and onset of MASLD where an increase in age is seen as the strongest epidemiological factor for MASLD, MASH, and fibrosis. This is shown with a marked increase in prevalence with age (Juanola et al., 2021). This strong correlation could be because elderly patients are more prone to possess alternative risk factors associated with MASLD such as hypertension, dyslipidemia, and diabetes (Gerges et al., 2021). The effect of gender on risk of development is rather controversial. It was first thought that mostly women were

afflicted by this disease, but many studies throughout the years have shown an unclear association between gender and prevalence (Gerges et al., 2021; Juanola et al., 2021). A study by Ayonrinde et al., showed that men had more adverse phenotypes (Ayonrinde et al., 2011). Studies by Ong et al. and Papatheodoridis et al. further proved this point when they found males had higher fibrosis and higher aspartate aminotransferase (AST) and ALT levels (Ong et al., 2005; Papatheodoridis et al., 2007). Ethnic and racial disparities in MASLD risk are multifactorial including but not limited to behavior, genetics, and socioeconomics. In 2016, Carr et al. analyzed various epidemiological studies and found that MASLD afflicted approximately 30% of the United States population, 32% of the Middle East population, 27% of Asian populations, 30% of South American population, 24% of European populations, and 13% of African populations (Carr et al., 2016). Within the United States, White and African Americans are seen to have the lowest prevalence whereas Hispanic Americans have the highest (Carr et al., 2016; Gerges et al., 2021).

Environmental risk factors include toxins, diet and lifestyle, smoking, and air pollution. Of these the most notable is diet and lifestyle increased intake and reduced activity create an imbalance that leads to obesity and insulin resistance that ultimately ends in a MASLD diagnosis. The Western diet includes an excess of carbohydrates, animal proteins, refined sugar, and additives that all contribute to obesity. Restaurants, fast foods, and numerous grocery stores lend a hand in the risk as they provide easy and quick access to low-nutrient, high sodium, and high fat foods. High fructose is known to activate DNL which can lead to inflammation. Excessive fats are delivered to the liver via the portal circulation where they are internalized by the hepatocytes increasing the

risk of steatosis. When diets, like the Western diet, are rich in lipids, carbohydrates, and proteins, post-meal blood glucose is higher. This in turn leads to a higher insulin secretion which also stimulates DNL further leading to hepatic steatosis. Many cases have shown that dietary intervention and exercise could very easily mitigate the risk associated with an unhealthy diet and lifestyle as well as reverse the effects of MASLD post-diagnosis (Gerges et al., 2021; Juanola et al., 2021).

### **Pathogenesis and Pathophysiological of MASLD**

Pathogenesis is the process by which a disease develops and how an individual becomes ill. Pathophysiology is the study of the effects of a disease, illness, or injury on the body. Gerges et al. defines pathophysiology as an interplay between metabolic, environmental, microbiome-related, and genetic factors which all also intertwine to describe the pathogenesis of a disease (Gerges et al., 2021; Powell et al., 2021). There is an immense amount of overlap in the understanding and mechanisms behind the two terms when discussing the progression of MASLD. Because of this overlap, different scientific papers use these terms interchangeable and therefore this thesis will discuss and summarize the two terms harmoniously.

There are two hypotheses typically used to describe the development and progression of MASLD. First is the two-hit hypothesis described by Gerges et al., that states there are two separate insults on the body that work together, in tandem to create an environment susceptible to the disease. The first hit leaves the body susceptible to a second insult that ultimately leads to the development to the disease. The first hit is an extreme accumulation of lipids in the liver caused by an unrestrained consumption of

fats, a sedentary life, obesity, and insulin resistance. The second hit is a metabolic insult such as inflammation and fibrogenesis (Gerges et al., 2021). Pouwels et al. attribute the two steps to different insults (Pouwels et al., 2022). The first hit being similar in that it focuses on fat deposition but different specifically stating this deposition leads to insulin resistance. The second hit expands on metabolic insults suggesting that cellular and molecular changes including oxidative stress and oxidation of free fatty acids in the liver are at fault. The excessive oxidation of overflowing fatty acids leads to cytokine injury, hepatic iron accumulation, and extracellular variation that all contribute to the disease (Pouwels et al., 2022). The second hypothesis is known as the multiple-hit hypothesis where many factors contribute to disease development at the same time. These factors include both environmental ones such as unhealthy, high-calorie diet, and genetic ones that lead a patient to be predisposed to insulin resistance, obesity, adipose tissue dysfunction, and an altered intestinal microbiota (Gerges et al., 2021).

Regardless of these differing hypotheses, the primary driver of MASLD pathogenesis is overnutrition that leads to adipose deposits and ectopic fat accumulation. In this environment macrophages begin to infiltrate fostering a pro-inflammatory response that leads to insulin resistance. IR creates a setting where lipolysis is no longer inhibited and inappropriately increases the delivery of fatty acids to the liver and DNL. These processes combine to overwhelm the metabolic capacity of the liver. The imbalanced and overwhelmed lipid metabolism causes the formation of lipotoxic lipids which induce cellular stress, inflammasome activation, and apoptotic cell death. This in

turn leads to inflammation, fibrogenesis, and the activation of tissue regeneration (Powell et al., 2021).

As mentioned previously, MASLD is marked by the accumulation of hepatic lipids, steatosis, in more than 5% of hepatocytes. Many issues contribute to the onset of hepatic steatosis including insulin resistance, obesity, and adipose tissue dysfunction. Some of these factors are shown in figure 4. As discussed in the fatty acid metabolism section, insulin resistance is the weak biological response to glucose uptake even when insulin levels are normal. Under normal conditions, insulin has many functions; it encourages glucose uptake in skeletal muscles and the liver, it synthesizes TGs and inhibits lipolysis in AT, and it stimulates DNL to synthesize TGs and suppresses glucose production in the liver. When there is systemic IR, the pancreas secretes more insulin aid in the peripheral glucose uptake issue and to suppress glucose production in the liver. When there is IR that affects AT, lipolysis is not inhibited causing an increase in FFA delivery to the liver. This increase delivery leads to the accumulation of lipid metabolites and FFAs in the liver cells. These two processes activate serine/threonine kinases such as protein kinase C, c-JNK, and IKK- $\beta$  allowing them to phosphorylate the insulin receptor or insulin receptor substrate. Because this is not a normal process it interferes with tyrosine phosphorylation and disrupts insulin signaling eventually leading to hepatic IR. When the liver is unable to respond to insulin there is a decrease in glycogenesis and an increase in gluconeogenesis causing hyperglycemia and hyperinsulinemia that further exasperate the issue. Interestingly, DNL is not suppressed and actually increased which increases the delivery of FFAs to the liver. The insulin resistance and its downstream

effects lead to steatosis and an increase in the secretion of VLDL which both cause a larger lipid load to reach AT. As will be discussed shortly, the AT cannot store these lipids in droplets as it is dysfunctional and overwhelmed so they in turn are delivered to the liver again. Once the liver cells are overloaded and exposed to lipotoxic bioactive lipids there is further insulin signal impairment, oxidative damage, inflammation, and fibrosis (Carr et al., 2016; Gerges et al., 2021). Insulin resistance ultimately leads to the buildup of lipids in hepatocytes and without its resolution its negative consequences can lead to the progression to MASH.

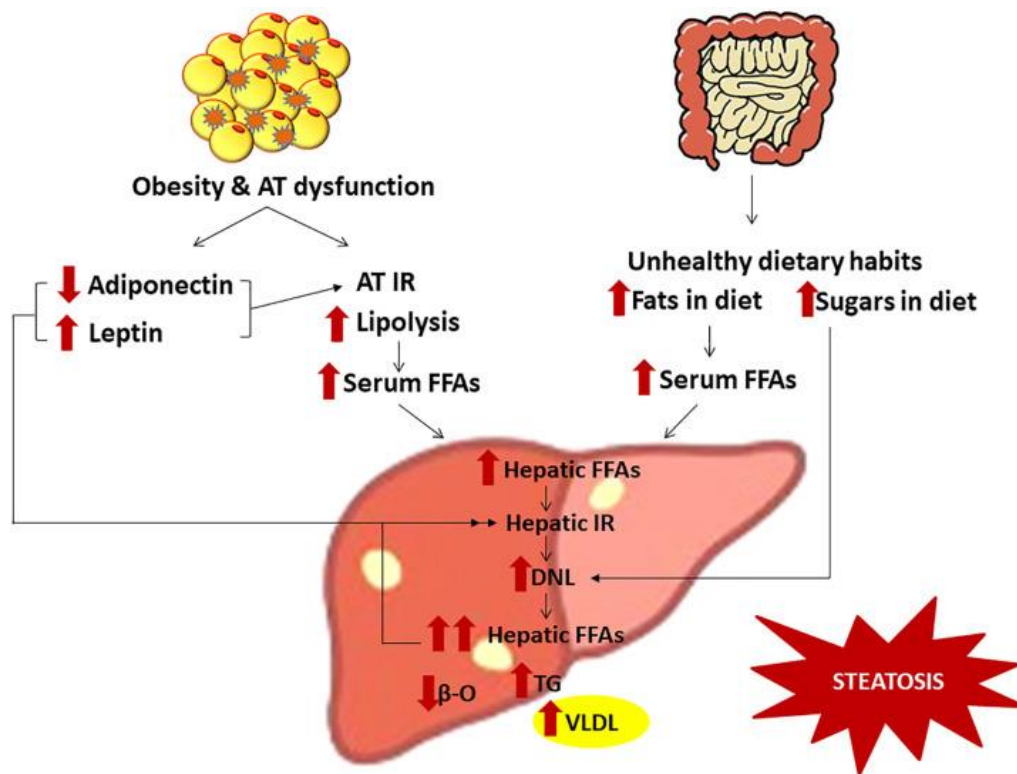


**Figure 4:** The factors involved in hepatic fat accumulation (Gerges et al., 2021).

AT dysfunction and obesity both play an important role in steatosis development.

AT is an endocrine organ that secretes hormones and adipokines that travel through the

bloodstream to elicit responses at downstream organs. Adiponectin is a cytokine secreted by AT that is hepatoprotective by increasing hepatic sensitivity to hepatic insulin. It does so by suppressing glycogenolysis and lipogenesis and increasing glucose use to help hepatic IR. It also has antifibrotic, anti-inflammatory, anti-obesity, and antioxidant properties. It is implicated in steatosis development as it decreases as fat cell size and IR increase and in chronic metabolic diseases. An adiponectin deficiency leads to further IR, obesity, and mitochondrial dysfunction. Leptin is another cytokine released from AT that acts as a hormone playing a role in body weight and fat content regulation. It acts centrally to decrease consumption, increase energy use, and to prevent lipid accumulation. Obese and patients with MASH typically have leptin resistance that decreases glucose uptake and increase gluconeogenesis which leads to hyperglycemia and IR development. It also has a pro-inflammatory effect in excess (Carr et al., 2016; Gerges et al., 2021). Since both of these AT cytokines have hepatoprotective effects, their loss is detrimental to the maintenance of a healthy hepatocyte environment leaving them susceptible to steatosis development. Obesity also leads to steatosis in that it causes lipid accumulation in adipocytes, enlarging the cell size and activating c-JNK and IKK- $\beta$  inflammatory pathways. These pathways, as mentioned, decrease AT sensitivity to insulin which in turn increases lipolysis through its dysfunctional antilipolytic effects. Hyperinsulinemia and hepatic IR aggravate AT inability to store fats as lipid droplets since they both increase DNL in hepatocytes which increases the circulation of TGs delivered to the AT (Gerges et al., 2021).

Many factors contribute to simple steatosis progressing to MASH such as lipotoxicity, inflammation, cytokines, and oxidative stress. Inflammation and inflammatory cytokines create histological damage such as necrosis, neutrophil infiltration, and the production of Mallory bodies that aid in the progression from simple steatosis to MASH. AT dysfunction, obesity, and IR lead to the activation of inflammatory pathways such as c-JNK and NF- $\kappa$ B that release TNF- $\alpha$  and IL-6 that elicit an inflammatory environment for other organs, such as the liver. A decrease in adiponectin from dysfunctional AT removes the inhibition on NF- $\kappa$ B pathways so there is no protection against inflammation. An inflammatory environment is also known to aggravate IR since TNF- $\alpha$  and IL-6 stimulate lipolysis and an increase in serine/threonine phosphorylation of IRS through c-JNK activation. IL-6 itself suppresses IRS and the GLUT-4 transporter as well as downregulated PI3K which also leads to an increase in IR (Gerges et al., 2021).

Lipotoxicity is the harmful accumulation of toxic lipid species that leads to chronic inflammation and steatosis progression to MASH. In lipid excess AT is unable to act as the main storage center and lipids begin to accumulate where small stores are found such as in the liver, muscles, and heart. The accumulation in tissues that are not suited for storage induces lipotoxicity. The main lipids that accumulate in the liver, TGs from DNL, are actually seen to be protective rather than lipotoxic. It is the excessive delivery of FFAs and other lipotoxic species to the liver via the portal circulation from the GI tract and AT that leads to lipotoxic dysfunction. Saturated FAs such as palmitic acid, compared to unsaturated FAs have more severe pathogenic effects that can push simple

steatosis to MASH (Bence & Birnbaum, 2021). Overall, the excess of toxic lipid species and the liver's constant exposure to them leads it susceptible to injury allowing disease progression to occur.

Oxidative stress is the disturbance of the pro-oxidant and antioxidant balance that favors the pro-oxidant side through an increase in ROS or a decrease in antioxidants. Oxygen has a chief role in creating oxidative stress because of its ability to accept electrons forming radicals such as hydroxyl radicals, nitro oxide radicals, and superoxide anion radicals. These occur via unstable reactions during normal metabolism and negatively react with biological compounds. Endogenous reactive oxygen species (ROS) arise from processes that contribute to lipid metabolism such as mitochondrial  $\beta$ -oxidation and peroxisome breakdown. The mitochondrion of the cell is the most important energy supply that consumes and produces most of the oxygen and therefore makes the most ROS. In the transition from steatosis to MASH the overload of FFAs leads to electron leakage during mitochondrial  $\beta$ -oxidation that causes an excess of ROS to be produced. TNF- $\alpha$ , a cytokine commonly released in MASH patients, and lipid peroxidation products are known to inhibit the electron transport chain (ETC) and deplete mitochondrial cytochrome c which exasperates mitochondrial dysfunction and leads to the production of more ROS. These ROS then damage the mitochondrial membrane decreasing  $\beta$ -oxidation of lipids causing them to accumulate more. To compensate for the damage to mitochondria, Peroxisome Proliferator-activated Receptor alpha (PPAR- $\alpha$ ), abundant in the liver, is activated by FFAs and localized to the inner mitochondrial membrane. This increases ETC activity and therefore limits the ability of ROS to form

with the consequence of uncoupling the ETC from ATP synthesis leaving the cell vulnerable to ATP depletion eventually ending in necrosis (Gerges et al., 2021; Koek et al., 2011).

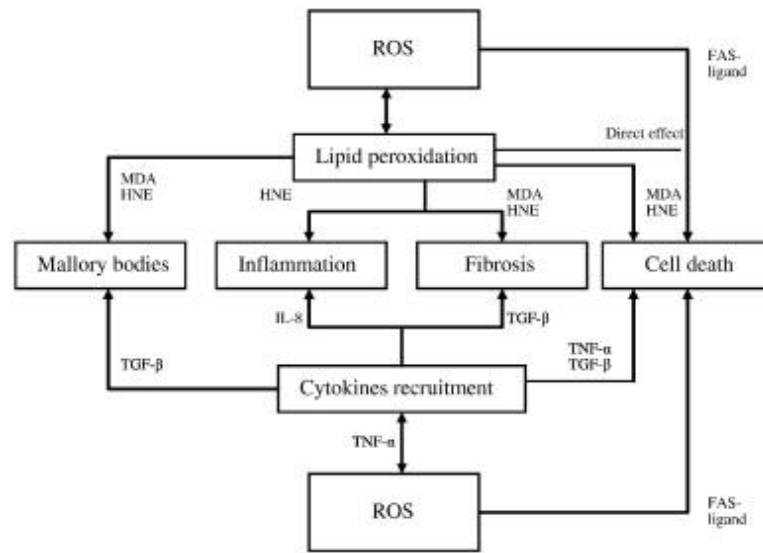


**Figure 5:** OS Liver Injury in MASH (Koek et al., 2011)

Another key player in the production of ROS are microsomes which are small vesicles that contain enzymes such as Cytochrome P450 enzymes, CYP2E1, and CYP4A. Cytochrome P450 is responsible for the metabolism of FAs, cholesterol, bile acids, and exogenous compounds. CYP2E1 and CYP4A are both key enzymes in the lipo-oxygenation of long-chain fatty acids to prevent their toxic effects. In doing so, however, they produce reactive oxygen species that further increase the oxidative stress in the cell. As mentioned in the fatty acid metabolism section, peroxisomes aid in FFA breakdown to acetyl-CoA that is transported into the mitochondria to be degraded. This process produces hydrogen peroxide, a highly reactive hydroxyl radical, and with an overflow of FFAs it creates even more oxidative stress. Lipid peroxidation occurs when these ROS

reach with the hydrogen atom of an unsaturated FA. By doing so a chain reaction is created that produces a heterogeneous group of lipid peroxides capable of disrupting membranes and producing reactive metabolites that cause cell dysfunction (Koek et al., 2011). Again, the increase of FA availability seen in simple steatosis and MASH patients leads to increase in these detrimental processes that push a patient along the progressive path of the disease.

Inflammation and inflammatory cytokines create histological damage such as necrosis, neutrophil infiltration, and the production of Mallory bodies aid in the progression from simple steatosis to MASH. AT dysfunction, obesity, and IR lead to the activation of inflammatory pathways such as c-JNK and NF- $\kappa$ B that release TNF- $\alpha$  and IL-6 that elicit an inflammatory environment for other organs, such as the liver. A decrease in adiponectin from dysfunctional AT removes the inhibition on NF- $\kappa$ B pathways so there is no protection against inflammation. An inflammatory environment is also known to aggravate IR since TNF- $\alpha$  and IL-6 stimulate lipolysis and an increase in serine/threonine phosphorylation of IRS through c-JNK activation. IL-6 itself suppresses IRS and the GLUT-4 transporter as well as downregulated PI3K which also leads to an increase in IR (Gerges et al., 2021).

The buildup of ROS leads to oxidative stress (OS) liver injury where the antioxidant abilities of the liver are overwhelmed. Glutathione is a non-enzymatic example of an antioxidant that is responsible for detoxifying ROS from the mitochondrial ETC. When OS is present, glutathione reductase converts glutathione disulfide to glutathione. The consequence of this overwhelming oxidative stress is lipid

peroxidation, stellate cell activation leading to fibrosis, chronic inflammation, and apoptosis. ROS and lipid peroxidation, as discussed, directly damage the cell membrane, protein, and DNA. They also induce an inflammatory response by upregulating TNF- $\alpha$ , IL-1 $\beta$ , and IL-6. TNF- $\alpha$  is enhanced in MASH patients causing more lipid peroxidation that worsens the function of the mitochondrial membrane leading to more OS. TNF- $\alpha$  also leads to direct hepatocyte death via apoptosis and the formation of Mallory bodies. OS leads to Kupffer cell activation and death receptor fas-ligand expression causes necrosis, caspase activation, and death receptor mediated cell death (Koek et al., 2011).

The step following MASH development is fibrosis for which HSCs are responsible, which is shown in figure 6. Inflammatory cytokines, ROS, and dead cells cause MASH patients to develop fibrosis. Damage-associated molecular patterns (DAMPs) and ROS released from dead cells and leptin activate Kupffer cells making them release TGF- $\beta$  and IL-6 which are pro-fibrotic cytokines that activate HSCs. Damaged hepatocytes found in MASH patients also activate Kupffer cells which leads them to activate HSCs. The active HSCs express an increased  $\alpha$ -smooth muscle actin and release cytokine and chemokine that are pro-fibrotic. Upon activation, HSCs proliferate (transdifferentiate) into a contractile matrix releasing cell, a myofibroblast, that secretes extracellular matrix fibers and matrix remodeling enzymes. The major components of ECM that are secreted include collagen I and III that change the physical attributes and stiffness of the ECM and tissue. Changes induced by collagen I and III include impaired nutrient exchange, immune system and further HSC activation, and loss of fenestration (Gerges et al., 2021; Han et al., 2023).

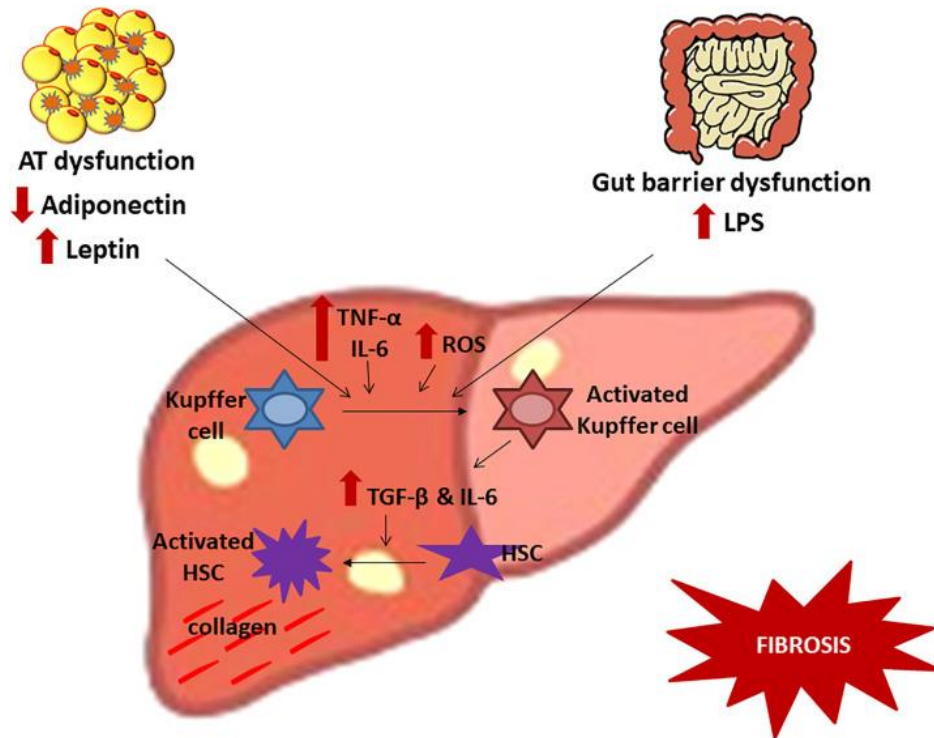


**Figure 6:** Progression from MASH to fibrosis (Gerges et al., 2021)

### Diagnosis and Stages of MASLD

There are various invasive and noninvasive techniques employed to diagnose and stage MASLD. This disease often is found coincidentally during routine medical examinations through radiological imaging or laboratory work as it can be asymptomatic until fibrosis and cirrhosis develop (Carr et al., 2016; Pouwels et al., 2022). Some noninvasive techniques include laboratory tests, evaluating clinical variables, and assessing biomarkers such as inflammatory and oxidative stress markers (Gerges et al., 2021). Routine laboratory work can show elevated aminotransferases such as ALT and AST which can suggest the presence of MASLD. ALT elevations are more prevalent than AST in MASLD whereas the reverse is true in MASH patients (Pouwels et al., 2022). The ratio of these two aminotransferases can sometimes predict a patient's risk of

developing MASH from simple steatosis (Gerges et al., 2021). It is controversial, however, to use these liver enzymes as diagnostic criteria as there is a limited amount of agreement on their elevation in patients with MASLD. One study found that 60% of MASLD patients have normal ALT levels and not have MASH or advanced fibrosis. Another study found that 53% of participants with elevated ALT levels do not have MASH or advanced fibrosis (Fracanzani et al., 2008; Verma et al., 2013). These inconsistencies suggest that it may be necessary to use other diagnostic methods.

Other non-invasive diagnostic methods include imaging techniques such as ultrasound, CT, and MRI. These methods are simply used to substantiate a diagnosis as they are unable to differentiate between the histological subtypes of simple steatosis and MASH or early fibrosis. The findings associated with MASLD include increase echogenicity on ultrasound, a decrease in hepatic attenuation on CT, and an increased fat signal on an MRI. MRIs are favorable because they can detect less than 5% of steatosis within the liver and could be beneficial to early detection to employ preventative measures (Carr et al., 2016; Pouwels et al., 2022). Since imaging methods can only aid in diagnosis and are unable to diagnose late stages of MASLD another method must be used, the liver biopsy.

The liver biopsy is the established benchmark for diagnosing MASLD which can assess the amount of hepatic damage and the severity of disease. Macrovesicular steatosis where there are large lipid droplets that push the nucleus of the cells to the side is required to diagnose the patients with MASLD. To diagnose a patient with MASH, one must find steatosis, lobular portal inflammation, hepatocellular injury, and ballooning

when a biopsy is performed. It is also possible to see mild fibrosis as abnormal ECM deposition, eosinophilic cells, and Mallory bodies. A liver biopsy allows a physician to grade the diseased tissue using the NAFLD Activity Score (NAS). The components are steatosis on a scale from 0 to 3, lobular inflammation on a scale from 0 to 3, and hepatocellular ballooning on a scale from 0 to 2. The overall score is used to make the final diagnosis with a 0 to 2 being NAFLD (now MASLD), a 3 to 4 being non-diagnostic, borderline, or NASH (now MASH), and a 5 to 8 being NASH (now MASH). This grading scale is critical for determining the progressive nature of an individual's disease; it is critical to assess the risk of morbidity and mortality which are dependent on the severity of histological findings. Although a biopsy is the gold standard, it has many limitations and is not recommended for all patients. Limitations include high prevalence of MASLD making it unrealistic to sample all suspected patients, risk of biopsy, low likelihood/percentage of progressive disease, sample bias, invasive nature, observer variability, misdiagnosis, and staging inaccuracies (Carr et al., 2016; Gerges et al., 2021; Pouwels et al., 2022). Liver fibrosis has the strongest correlation with liver-related morbidity and mortality so there are many simple scores used to assess disease severity. These include the NAFLD fibrosis score, Fibrosis-4 (FIB-4) index, and aspartate aminotransferase-to-platelet ratio index. Liver stiffness can also be measured via ultrasound-based elastography or magnetic resonance elastography (Powell et al., 2021). It is important to assess the degree of fibrosis within the liver early in the diagnosis process and these tests make that feat rather simple.

### **Management and Treatment Options**

There are currently no FDA-approved medications or treatments for MASLD (Gerges et al., 2021). Diet, weight loss, and lifestyle modifications are the most effective in decreasing a patient's risk of MASLD development as well as improving features of the disease if a patient has already been diagnosed. A healthy lifestyle approach can look like a reduced caloric intake, an increase in monounsaturated FAs, omega-3 FAs, fiber, and specific protein sources such as fish and chicken (Pouwels et al., 2022). A balanced diet and sustained exercise can reduce the amount of FFAs delivered to the liver as well as improve AT dysfunction, both which are cornerstones for MASLD and MASH improvement (Gerges et al., 2021). Some studies showed that a 5% loss of weight for MASL patients and 9% for MASH patients improved AST and ALT levels, the histology of the liver, and fibrosis (Carr et al., 2016). A study conducted by Vilar-Gomez et al. found that in 90% of patients who successfully lose more than or equal to 10% of weight had complete MASH resolution (Vilar-Gomez et al., 2015). If a patient's disease is severe or fast progressing or if lifestyle and pharmacological treatments are ineffective, Bariatric surgery may be necessary. Bariatric surgery can improve T2DM symptoms, induce weight loss, increase long-term survival, and allow fibrosis to regress. It also can improve metabolic complications and hepatic inflammation (Gerges et al., 2021; Pouwels et al., 2022).

Aside from lifestyle changes, patients can increase their exogenous antioxidant intake which has hepatoprotective effects. Vitamins, particularly Vitamin E, are a great example of a non-enzymatic antioxidant that has been successful in reducing hepatic

injury. Vitamin E is lipid soluble with free radical-scavenging properties allowing it to protect against ROS. In a study discussed by Pouwels et al. patients were given 800 IU/day of Vitamin E which successfully reduced steatosis, steatohepatitis, and ALT levels. Although helpful, long-term usage should be limited and it is suggested as a treatment only for biopsy-proven MASH patients (Gerges et al., 2021; Pouwels et al., 2022). Another powerful antioxidant is caffeine which has hepatoprotective effects in that it can ease the strain of oxidative stress and inflammation and improve liver enzyme levels. Polyphenols are a heterogeneous class of plant derived compounds that also have antioxidant properties. These compounds are contained in certain vegetables, fruits, tea, mushrooms, cereals, and spices (Pouwels et al., 2022). Resveratrol is a natural polyphenol extracted from red grapes that has both anti-inflammatory and antioxidant properties. It has shown to help with hepatocyte ballooning and steatosis, lower inflammatory and oxidative stress markers, and improve IR in high-fat-diet rats (Bujanda et al., 2008; Ding et al., 2017; Shang et al., 2008). Along with lifestyle modifications, daily consumption of this polyphenol can benefit IR and inflammation, ultimately leading to disease improvement.

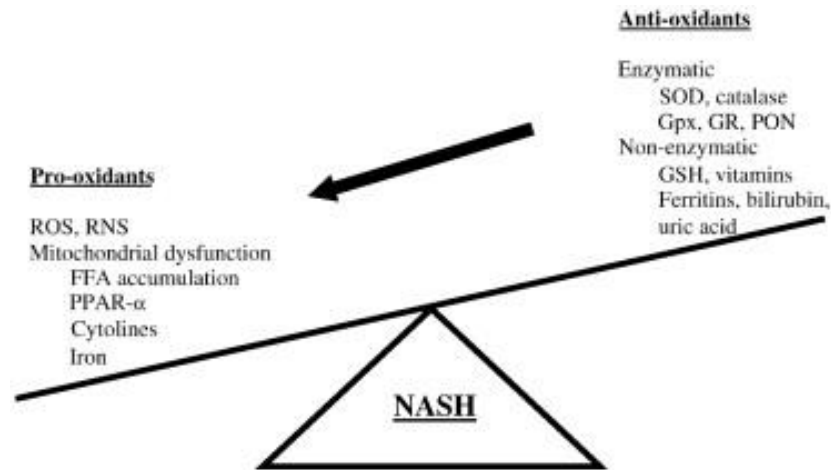


**Figure 7:** Balance between oxidants and anti-oxidants (Koek et al., 2011)

Although not FDA approved there are various pharmacological medications that can be prescribed to improve patient outcomes and risks associated with mortality and morbidity. Since there is a lack of FDA approval many studies suggest only using these treatments for patients with a high risk for progressive disease or those with progressive disease. Examples of medications used are Metformin, an insulin sensitizer, Pioglitazone, a PPAR- $\gamma$  agonist, GLP-1 analogues, an antidiabetic drug that aids in weight loss, and Statins, to help with dyslipidemia (Gerges et al., 2021; Powell et al., 2021). There are certain medications undergoing clinical testing to bridge the gap in treating this disease. A medication that is currently in phase 3 clinical testing to treat MASH with fibrosis is Resmetitrom. It is an oral liver-directed, thyroid hormone receptor beta-selective agonist (Harrison et al., 2024).

The most important part of MASH management is to mitigate the factors contributing to steatosis and systemic inflammation and to minimize cardiovascular risk. This can be done with a combination and optimization of many treatments used to treat

simple steatosis. These include, as mentioned, lifestyle changes such as diet and weight loss, daily antioxidant consumption, and pharmacological intervention (Powell et al., 2021).

### **SPECIFIC AIM**

Metabolic Dysfunction-Associated Liver Disease is one of the most predominant and destructive liver diseases of the Western World that causes chronic liver disease. There are currently, however, no FDA-approved treatments and regimes for MASLD, causing patients with progressive disease to have a poor outlook post diagnosis. The current treatments of diet and exercise, antioxidant supplements, and some medications help patients slightly but not significantly enough to resolve MASLD and its progression. The lack of approved treatments is due to the heterogeneous profile of the disease that includes numerous separate cell compartments and organs all interacting that creates an extremely difficult microenvironment to model. Current in vitro and in vivo models do not accurately and fully recapitulate the disease and its potential progressive nature. To address this issue this thesis aims to investigate the current disease models for MASLD and to propose a new model that could potentially allow for therapeutic investigation and implementation to treat this disease. It will investigate the 2D in vitro cell culture methods such as monoculture and organs on a chip. This thesis will also investigate 3D in vitro cell culture, including human-induced Pluripotent Stem Cell (hiPSC) derived organoids, multicellular organoids, and organoids from patient tissue. Many in vivo modeling techniques will be examined as well.

## EVALUATING THE MODELING TECHNIQUES FOR MASLD

MASLD is a progressive disease that involves many cellular compartments and different organs working together to create a heterogenous profile. This characteristic makes it rather difficult to establish a model that accurately and faithfully recapitulates all the aspects of this complex disease. In this section, various in vitro 3D models and in vivo animal models will be described to lay a foundation of understanding about the numerous methods of modeling MASLD.

Bronsard et al. modeled Metabolic Dysfunction-Associated Liver Disease using 3D multi-cell-type liver organoids. For the cell culture the study used progenitor HepaRG cells seeded at density of  $2 \times 10^6$  cells in a flask. HepaRG cells are capable of metabolizing drugs similarly to primary human hepatocytes. They also accumulate TGs and exhibit similar changes seen in MASH patients upon exposure to FAs. The HepaRG cell line can differentiate into hepatocytes and cholangiocytes. This model co-cultures HepaRG cells with primary human macrophages and HSC-derived LX-2 (Stellate cells) cells to form what they call HML organoids. The cells were cultured in William's E culture medium supplemented with 10% FBS, 2 mM glutamine, 50  $\mu$ M sodium hydrocortisone hemisuccinate, 5  $\mu$ g/mL insulin, 50 U/mL penicillin, and 50  $\mu$ g/mL of streptomycin. Two weeks post seeding the cells were cultured with the same medium supplemented with 2% DMSO that allows them to differentiate into cholangiocyte-like and hepatocyte-like cells. The human macrophages were extracted from peripheral blood mononuclear cells and plated in a flask. The cells were cultured in RPMI 1640 and supplemented with 100 IU/mL penicillin, 100 mg/mL streptomycin, 2 mM L-glutamine, 1 mM HEPES, and 10%

fetal bovine serum (FBS). The HML organoids were formed using the Sigma micromold system to mix ~2000 cells together per organoid. 80% of the cells were differentiated-HepRG cells, 10% were macrophages, and 10% were LX2 cells. They were cultured in a self-assembly medium which was William's E medium supplemented with 10% FBS, 2 mM glutamine, 50  $\mu$ M sodium hydrocortisone hemisuccinate, 5  $\mu$ g/mL insulin, 50 U/mL penicillin, and 50  $\mu$ g/mL streptomycin. After 3 days of the culture the FBS was reduced to 1% (Bronsard et al., 2024).

The HML organoids were treated with a mixture of FAs to induce steatosis and fibrosis. The mixture included 150  $\mu$ M stearic acid and 300  $\mu$ M oleic acid prepared with FA-free Bovine Serum Albumin (BSA). The mixture was given on day 5 after seeding and repeated every other day until day 14. Numerous processes were used to determine if these organoids were successful at recapitulating the disease profile. RNA was isolated using a nucleospin RNA isolation kit and a nanodrop 1000 system was used to quantify it. A high-capacity cDNA Reverse Transcription Kit was used to create cDNA from the isolated RNA via reverse-transcription. RT-qPCR with SYBR Green Master mix was used to detect and quantify specific RNA sequences. Tissue samples were harvested from the organoids, fixed with 5% formalin for 60 minutes, and washed in PBS. The cut slices were stained with heamalin-eosin-saffron (HES) reagent and labelled using rabbit anti-CYP3A4, mouse anti-cytokeratin 19 (CK19), and mouse anti-CD68, rabbit anti-Col1A1, mouse anti-COL4, and mouse anti-vimentin. The nucleus was stained using DAPI. Total lipid amounts were extracted and released FFAs were extracted as well. Only a small quantity of FAs was found so the study employed a very sensitive negative ion chemical

ionization gas chromatograph-mass spectrometry. The type of FAs in the sample were identified based on retention time versus an authentic standard and corresponding to specific ions formed. Lipids were stained using 1  $\mu$ M BODIPY™ 493/503 diluted in PBS for 30 minutes prior to fixing in 5% formalin and then mounted on a glass slide and imaged using the Leica DMI600 Inverted Microscope. Using ELISA kits, the study quantified the secreted cytokines in solution including IL-1 $\beta$ , IL-6, and TGF- $\beta$ . Apolipoprotein-B secretion was measured using an ELISA kit as well. Intracellular ATP was measured to assess cell viability using the CellTiter-Glo Luminescent Cell Viability assay kit. The results were given as a percentage of a control value (Bronsard et al., 2024).

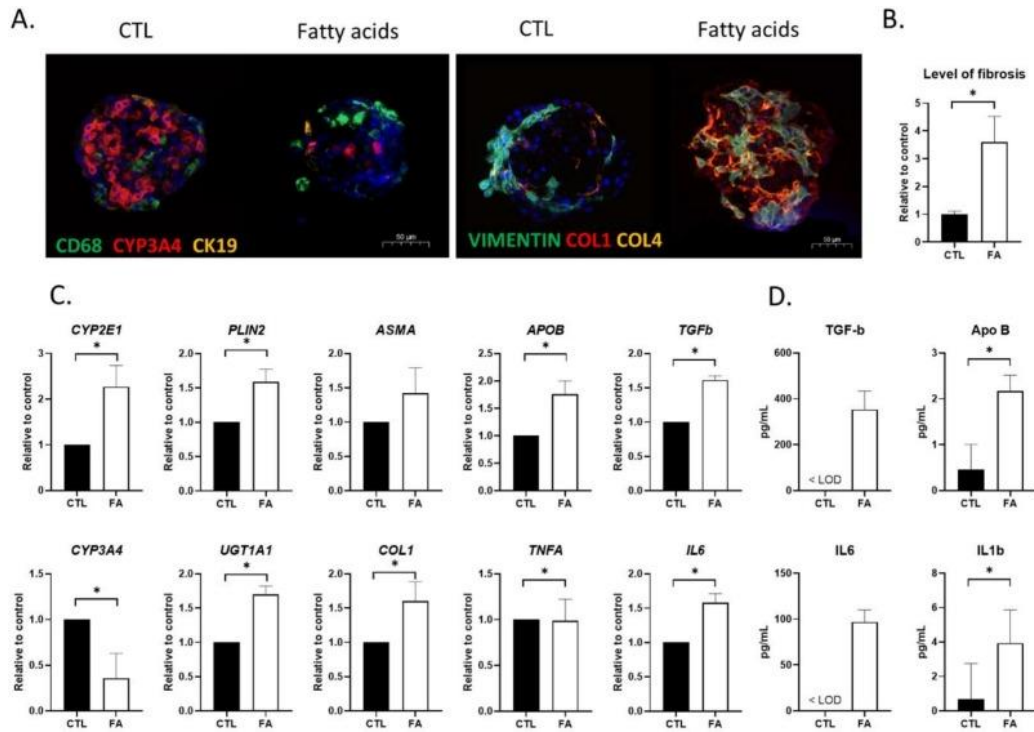


**Figure 8:** Characteristics of MASLD exhibited after FA exposure to HML organoids. (A) Labeling of CD68 (green), CYP3A4 (red), and CK19 (yellow). (B) Fibrosis quantification using COL1 staining. (C) Quantitative RT-PCR to assess expression of CYP2E1, CYP3A4, PLIN2, UGT1A1, ASMA, COL1, APOB, TNF- $\alpha$ , TGF- $\beta$ , IL-6 (Bronsard et al., 2024).

The various investigative methods showed that HML organoids expressed liver markers, maintained the differentiation-associated marker expression, and upregulated the expression of xenobiotic-metabolizing. For the expression of liver markers, organoid samples were harvest at days 5, 7, 10, and 14 of culture. CYP3A4 immunohistochemistry staining showed the organoids exhibit a normal appearance to hepatocytes which are large, polygonal cells spread throughout the tissue. Staining for the epithelial marker, cytokeratin 19, showed there were cholangiocyte-like cells in the outer region of the organoid. Stellate cells were found to self-organize and spread over the 14-day period of culture. There was also proof that M1 macrophages with pro-inflammatory properties

remained differentiated throughout the process in that they were CD68-positive. Two differentiation markers, Hepatocyte Nuclear Factor-4 alpha (HNF-4 $\alpha$ ) and Albumin were upregulated between day 7 and 10 and between day 5 and 7, respectively. Both of these markers remained high until day 14. The expression of phase 1 and phase 2 xenobiotic metabolizing enzymes like CYP2E1, CYP3A4, and UGT1A1, were increased over time. A phase 3 transporter, MRP2, was unchanging over time and correlated with the polarization of the hepatocyte canalicular membrane and the cholangiocyte apical membrane (Bronsard et al., 2024).

The FA mixture administered from day 5 to 14 to the HML organoids induced steatosis within them. After these 9 days of exposure there was an increase in neutral lipid droplets within the organoids. BODIPY™ staining and total TG count were higher than the control. GC-MS analysis showed saturated and monosaturated FAs with a low amount of poly-unsaturated and n-3 FAs in the control. On the other hand, post FA treated organoids found that C18:1 n-9 FAs accumulated more than other ones. The FA treated HML organoids also presented features of MASLD. There was a larger production of COL1 and COL4 and higher expression of COL1A1, which are responsible for fibrosis. CYP3A4 was lower while CYP2E1 and UGT1A1 were higher. Lipid-metabolism-related genes such as PLIN2 (a lipid droplet coating protein) and APOB as well as lipid secretion levels were greater compared to control. There was an increased secretion of pro-inflammatory and pro-fibrotic cytokines like IL-1 $\beta$ , IL-6, and TGF- $\beta$  (Bronsard et al., 2024).

This study was successful, as shown in figure 8, in creating an organoid system that included the major cell types present in the human liver. This system was composed of HepaRG cells differentiated into both cholangiocyte-like and hepatocyte-like cells as well as Macrophages and Stellate cells. Their HML organoids were effective models of MASLD and even were pathologically relevant in that it allowed them to perform further testing relating to the disease. The mixture of stearic and oleic acids amplified lipid buildup and metabolic dysfunction as well as induce mild inflammation and a pro-fibrotic response. The latter two results are similar to those seen in steatohepatitis suggesting this model may be useful in exhibiting long-term disease progression.

Gwag et. al established two MASH models, one in vivo method using mice and an organoid model. This study focused on testing the therapeutic potential of CD47 or its ligand Thrombospondin 1 (TSP1) since there are protective affects against obesity-associated MASLD when these are missing. However, for the purpose of this thesis, the bulk of what will be investigated is the MASLD model prior to anti-CD47 antibody treatment.

The mice in the study conducted by Gwag et al. were held in a pathogen-free environment with a light-dark cycle that mimic the natural environment. To induce MASH the mice were feed an AMLN diet for 20 weeks. This diet was composed of 40% kcal from fat, 20% kcal from fructose, and 2% kcal from cholesterol. The second method was creating a 3D human MASH organoid model. Their organoids were composed of human hepatocytes, THP1 derived macrophages, and human stellate cells. The cells were seeding at 3,000 cells/well at a ratio of 4:1:1 which is similar to the cellular distribution

seen in the liver. The organoids were given a MASH inducing media which was a DMEM media containing 1% BSA, 0.5 mM palmitate, 30 mM high glucose, 2  $\mu\text{g}/\text{mL}$  lipopolysaccharide (LPS). This media was used for 5-10 days to mimic the proinflammatory and pro-fibrotic environment seen in MASH (Gwag et al., 2022).

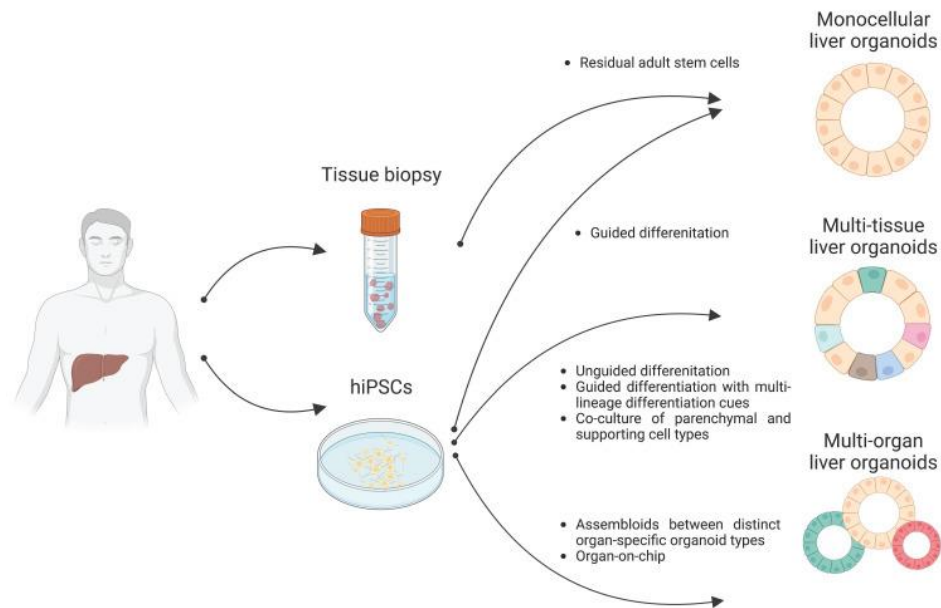
To confirm that this model successfully recapitulated MASH, many methods were employed including histological analysis, immunohistochemical staining, a lipid analysis, blood parameter analysis, and more. To analyze the histology of the liver samples they were fixed in 4% neutral buffered formalin and embedded in paraffin. The samples were then stained with Hematoxylin and Eosin (H&E), Masson's trichrome, and Sirius red and evaluated for fatty changes, inflammation, and fibrosis. The tissue sections were then deparaffinized and rehydrated for immunohistochemical staining. After blocking, they were incubated with CD11b-Alexa 647 antibody (a macrophage marker), washed, and mounted with DAPI and then imaged using a fluorescent microscope. The sections were also stained with anti-Collagen I antibody, anti-F4/80 antibody, or anti-neutrophil antibody, then incubated with a biotinylated secondary antibody and counterstained with hematoxylin. After image acquisition, neutrophils were counted and collagen I positive staining areas were determined. To analyze the lipid content of the tissue and subject, total plasma cholesterol and triglyceride concentration was found as well as the hepatic content of the two. A blood parameter analysis was performed on the mice to assess liver function using ALT and AST levels, blood glucose levels using a glucometer, and plasma insulin levels using an ELISA kit. A portion of the liver organoids were fixed with 4% paraformaldehyde (PFA) and stained with 0.5% Oil Red O in 60% isopropyl alcohol to

image lipid accumulation. To determine TG level of the organoids, another portion was lysed in 100  $\mu$ L of chilled Krebs Ringer Phosphate buffer and then the TG levels were measured enzymatically. RNA was isolated from both the mice livers and organoids and qPCR analysis was performed to assess the gene expression of inflammatory and fibrosis-related genes. SYBR green was used for the RT-qPCR test and relative mRNA expression was revealed (Gwag et al., 2022).

This study was successful in inducing advanced stages of MASLD that include MASH and fibrosis. The mice, after consuming the AMLN diet, developed obesity, T2DM, and MASH features. Their liver was increased in size and their total and free cholesterol levels, ALT levels, as well as their hepatic lipid and TG levels were elevated. The liver lipid metabolism-related genes, FASN, SCD-1, ACC, Shrepb1c, HMGCR, and HMGCs were upregulated. There was evidence of steatosis seen with Oil Red O staining and fibrosis seen with Trichrome and Sirius red. There was also an increase in positive fibrogenesis regulator genes such as Timp1 and proteins such as  $\alpha$ -SMA and Collagen I. The organoid model, after MASH inducing medium treatment, had increased expression in IL-1 $\beta$ ,  $\alpha$ -SMA, and Collagen I. Both models successfully exhibited marked changes in MASH features, such as a reduction in liver immune cell infiltration, inflammation, and fibrosis, upon treatment with anti-CD47 antibody. (Gwag et al., 2022). These two models, the mouse model and organoid model, were successful at recapitulating key features of obesity-induce MASH, from simple steatosis to inflammation and fibrosis. The model's capacity to show altered features once MASH was induced makes them viable for various therapeutic testing.

Han et al. provides a review of novel platforms for modeling the pathophysiology of MASLD and MASH using 3D multicellular aggregates with liver-tissue like structure and enhanced performance compared to current methods as shown in Figure 9. Organoids can be generated from pluripotent stem cells, multipotent tissue-specific stem cells, or a tissue biopsy with adult stem cells or differentiated cells. This review investigates liver organoids from primary tissues and human pluripotent stem cells (hPSCs). For hepatocyte or cholangiocyte organoids generated from primary tissue, researchers must obtain primary hepatocytes or cholangiocytes by either mincing primary human liver tissues or using single-cell dissociation techniques. By doing so, one can generate organoids that have tissue-specific characteristics and are self-renewing. Cholangiocyte organoids (COs), more specifically intrahepatic COs, express cholangiocyte markers and progenitor and hepatocyte markers. This means they are capable of dynamic cellular plasticity and therefore can, with specific differentiation factors, develop into the two main cell types of the liver. In doing so an organoid that more authentically represents the cellular diversity of the liver is generated. Along with being structurally sound, ICOs exhibit mature hepatocyte features and functions such as albumin secretion, bile acid secretion, and glycogen storage. Hepatocyte organoids (HOs) exhibit morphology and gene expression similar to hepatocytes. They also possess bipotential transdifferentiation capacity meaning they can differentiate in hepatocytes or cholangiocytes. Human derived HOs are even more favorable as they have a self-renewal capacity and can be used for long-term expansion (Han et al., 2023). ICOs and HOs possess many characteristics that make them promising options to model MASLD and its progression.

Pluripotent stem cells either from embryonic stem cells or induced pluripotent stem cells are an alternative source to creating organoids. PSCs, using a guided differentiation protocol, will produce cells from a single germ layer. Organoids from PSCs have the potential to allow patient-specific disease modeling and drug discovery. Monocellular liver organoids from PSCs have been shown to stably expand and exhibit hepatic functions. PSC-derived COs function similarly to primary tissue COs making them an alternative since primary tissue may be difficult to obtain. These organoids also exhibit an interconnection between hepatocytes and cholangiocytes with a compact liver core bordered by biliary cysts that are both functional. This interconnection is aided by the bile canaliculi network that is established in these organoids. Multi-tissue liver organoids from PSCs are created using a highly defined differentiation protocol since the development of the liver in humans is quite complex. To differentiate into hepatocytes or cholangiocytes the cells must first be induced to endoderm and then to hepatoblasts. Non-parenchymal cells are derived from mesoderm. Multi-tissue liver organoids can be generated via co-culture of iPSC-derived hepatic endodermal cells with human umbilical vein endothelial cells and mesenchymal stem cells. They also can be generated by connecting the differentiation of PSCs into many germ layers (Han et al., 2023). This review examines two different 3D modeling systems that are equally capable and successful at modeling the complex structure and function of the liver. This lends them to being a viable option to model MASLD.



**Figure 9:** Depicting types of liver organoids such as monocellular liver organoids, multi-tissue liver organoids, and multi-organ liver organoids made from tissue biopsy or hiPSCs (Han et al., 2023).

Mukherjee et al. carried out a study to develop and validate an *in vitro* 3D model of MASH, specifically with a severe fibrotic phenotype. They co-cultured primary human hepatocytes with hepatic stellate cells, Kupffer cells, and endothelial cells using the InSphero 3D InSight™ three-dimensional human liver microtissue (3D-hLMT) system. 3D-hLMTs have a 5-week survival limit and can be used to exhibit ATP level, albumin secretion, human liver gene expression, histology, and the expression of bile salt export pump (BSEP). They are also successful at acting as an *in vitro* model of liver fibrosis. In MASH, disrupted hepatic architecture, vascular structure, and aberrant regeneration is ultimately what leads to mortality. This stage of the disease is reached when there is a high amount of unsaturated FFAs that accumulate and damage hepatocytes leading to cell death. This cell death, as previously discussed, activated Kupffer cells which in turn

activate HSCs to transdifferentiate into myofibroblasts leading to fibrosis (Mukherjee et al., 2019). This study aimed to model these features of MASH and how it is reached via exposure to loads of unsaturated FFAs, finding that palmitic acid (PA) most robustly exhibited the desired phenotype.

The 3D-hLMTs were cultured in 70  $\mu$ L of fresh hLiMM TOX medium at 37°C in 5% CO<sub>2</sub> for four days. The media was changed 24 hours later and treated with 0.5 M palmitic acid (from a 10 mM stock) which was repeated for two days. The final volume for hLiMM TOX treatments was 50  $\mu$ L. The experiment was ended on day nine where the supernatant was collected for ELISA kits and the tissues were lysed for RNA extraction. Taqman Real-time PCR (RT-PCR) was used after RNA was extracted using ReliaPrep RNA Miniprep system and cDNA was made using a reverse transcription kit. The DeltaCt method was employed to calculate mRNA expression normalized to GAPDH, B2M, and RPL30. ELISA kits allowed the measurement of ProCol1, P1NP, PIIINP, and PAI-1 from the supernatant. The liver microtissue supernatant IL-8 levels were measured using Luminex. Cell death and lysis were measured to assess cell cytotoxicity using the LDH activity released into the supernatant. Masson's trichrome staining was used to histologically evaluate the tissue sections (Mukherjee et al., 2019).

The palmitic acid treatment successfully triggered tissue damage and a pronounced fibrotic phenotype in the 3D-hLMTs. The high concentration of PA proved to be hepatotoxic inducing lipoapoptosis of the parenchymal cells of the liver leading to an inflammatory response. This inflammatory response created an environment that activated HSCs leading to fibrosis. The RT-PCR tests showed there was an increased

expression in collagen genes such as  $\alpha$ -SMA, fibronectin, TIMP1, PDGFR- $\beta$ , and PAI-1. PDGFR- $\beta$  is a marker of hepatic stellate cell activation showing that they are able to lay down ECM now. PAI-1 is a downstream target of TGF- $\beta$  proving that pro-fibrotic pathways were upregulated. These genes increased the level of active collagen synthesis which was shown by the presence of P1NP and PIIIINP. These are product of procollagen I and procollagen 3 synthesis, two precursors to collagen I and III. Presence of elevated IL-8 levels show that a proinflammatory microenvironment was created after PA treatment. The fibrosis development led to microtissue damage which was exhibited by the increased LDH levels in the supernatant of the organoids (Mukherjee et al., 2019). This study further validated effectively modeled MASH with a severe fibrotic phenotype by treating them with a clinical trial drug known to decrease MASH features. Since this drug allowed the phenotype to regress toward control features in the organoids, it was evident that they possessed the MASH features in the first place.

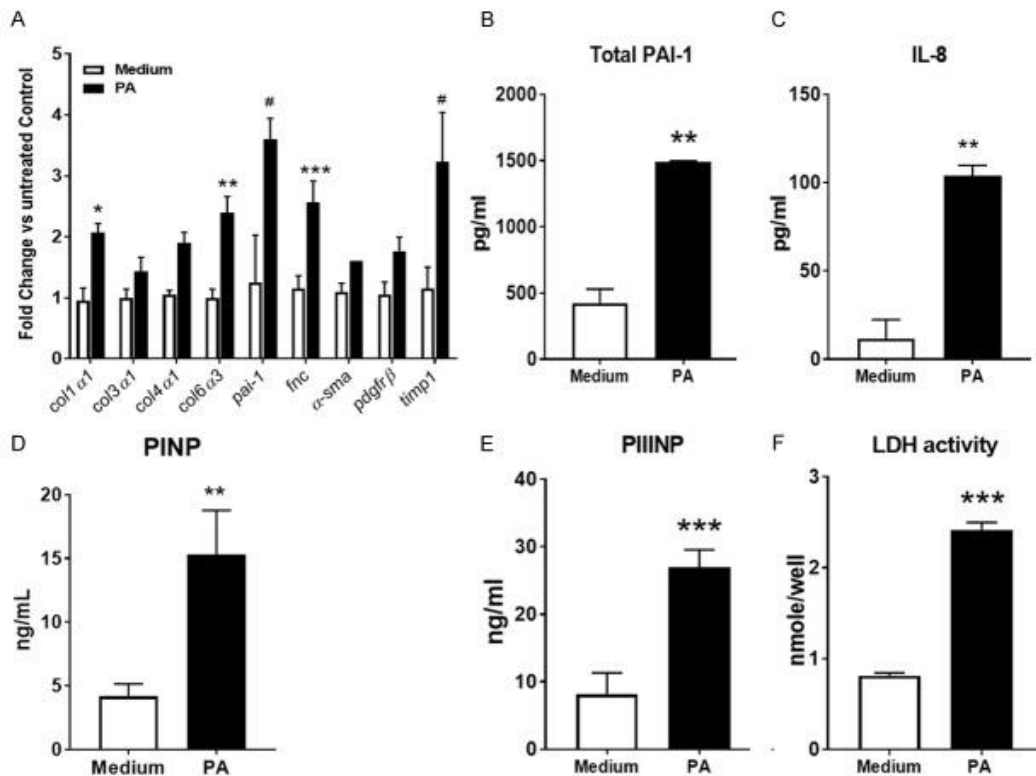


**Figure 10:** Profibrotic and proinflammatory makers induced in 3D-hLMTs after PA treatment. (A) RT-PCR quantification of profibrotic gene expression. (B and C) ELISA and Luminex measure for total PAI-1 and IL-8, respectively. (D and E) ELISA quantification of P1NP and PIIINP respectively. (F) LDH activity measured in supernatant (Mukherjee et al., 2019).

A study performed by Elbadawy et al., set out to investigate the efficacy of modeling MASH using organoids from primary liver tissue extracted from different stages of MASH mouse models. There were 4 groups of mice used in the study: the control, NASH A mice, NASH B mice, and NASH C mice. NASH groups A, B, and C represented mild, moderate, and severe phenotype of MASH, respectively. The mice were fed a methionine- and choline-deficient (MCD) diet to induce MASH features. NASH A mice were fed this diet for 4 weeks, NASH B for 8 weeks, and NASH C for 12 weeks. A 4 week diet of standard pelleted food was fed to the control mice. After

ethanasia of the mice, blood samples were collected, centrifuged to separate the serum, and used to analyze ALT, AST and total cholesterol levels. The livers were weighed, and tissue was collected from them for further experimentation. This liver tissue was minced into 0.5 mm<sup>3</sup> slices, digested in a 15 mL tube with prewarmed DMEM media containing 0.125 mg/mL of both collagenase type II and dispase II solution, and then incubated in a shaking water bath and pipetted every 15 minutes. It was then transferred through a 70 µm cell strainer, centrifuged at 600g, and the pellet was suspended in PBS and centrifuged again. This pellet of hepatocytes was then suspended in Matrigel in a 24-well plate with 0.5 mL/well of stem cell-stimulated media added. The media was changed 3 times a week (Elbadawy et al., 2020).

Tests were performed to assess the level of MASH within each mouse model. H&E staining was used to assess the severity of MASH of the degrees of hepatocellular steatosis, inflammation, ballooning, and hepatic fibrosis. Oil Red O staining was performed by fixing the organoids with PFA for 1 hour, dehydrating them with 30% sucrose overnight, embedding them in OCT, and freezing them. They were then washed with DI water, treated with 60% 2-propanol for 1 minute, and finally stained with Oil Red O for 15 minutes. This stain was used to image accumulation within the hepatocytes. Masson's trichrome stain was used to image fibrosis. Other tests and imaging techniques performed along standard protocols include immunofluorescence staining, quantitative RT-PCR, RNA sequencing, and immunohistochemical staining (Elbadawy et al., 2020).

The MCD diet-fed mice successfully modeled various levels of MASH progression. There were macroscopic changes in the liver appearance seen through the

different imaging technique. The weight of the liver in the more severe disease groups, NASH B and C, was greater than the control group. ALT levels in all three mice groups were higher. Interestingly, the body weight of the MASH mice was lower than the control. The mice also exhibited MASH features such as macro- and micro-vesicular steatosis, inflammatory cell infiltration, hepatocellular ballooning, and pericellular fibrosis. The Masson's trichrome staining and Oil Red O staining were positive for collagen and lipid deposition, respectively (Elbadawy et al., 2020).

After MASH disease progression was confirmed in the mice using the techniques describe above, liver organoids were generated from the tissue. The control mice and NASH A mice organoids formed from days three to seven and were cystic and large. The NASH B and C organoids formed later from days seven to fourteen into smaller spheroids with NASH C organoids exhibiting mesenchymal to epithelial transition. To confirm that the organoids contained the cellular components of the liver, immunofluorescence was performed. Normal hepatic markers such as Albumin, Alpha-fetoprotein, and CYP3A4/5 were present. HSC markers, which play a role in collagen deposition and therefore fibrosis, such as  $\alpha$ -SMA and vimentin, were also upregulated in NASH B and C. Collagen I was upregulated in NASH B and C confirming fibrosis progression. The study also assessed and compared the efficacy of formation for each MASH organoid group. There were functional differences seen between control and MASH mice insinuating that there were alterations in the MASH mice. Five days after seeding the same number of cell NASH A organoids were larger than B and C, but the number of B and C organoids compared to the control and A was increased. The

expression levels of inflammatory cytokines such as TNF- $\alpha$ , IL-1 $\beta$ , and IL-6 were used to investigate the mechanisms responsible for these differences in size. IL-1 $\beta$  was markedly increased in MASH compared to the other organoids leading the study to suggest that it is this cytokine that was promoting the large size of the NASH A organoids (Elbadawy et al., 2020). Overall, this study showed that earlier stages of mouse modeled MASH are more efficaciously modeled using organoids than later, more severe stages. These organoids prove helpful in modeling the disease and provide a resource for testing therapeutic methods.

McCarron et al. investigated a similar method of organoid formation but instead of mice livers they used irreversibly damaged livers from patients with MASH. These liver samples consistently gave rise to long-term expandable bipotent ductal organoids ready for hepatic differentiation that reproduce key functional characteristics of patient-specific MASH pathology. To obtain the tissue from patients, a liver biopsy from the peripheral liver edge was taken. To split and passage the tissue, organoid culture droplets were transferred to a 15 mL tube with cold basal medium, incubated on ice, and pipetted up and down. 2 mL of cold basal medium per well was added, the samples were mixed and spun, and then the basal medium was removed. Then they resuspended the pellet in fresh basement matrix and seeded it onto a suspension plate. The organoids were differentiating by adding bone morphogenic protein 7 for 5 days before changing to complete differentiation medium. After 11-14 days in this medium the organoids were ready for assessment. RNA was isolated from the tissues using Trizol and an RNA-sequencing library was prepared and analyzed. The study performed various tests that

assessed albumin secretion, ammonia degradation, and cytochrome p450 3A4 activity to analyze the organoids. They also induce apoptosis and lipid accumulation using PA and oleic acid (OA) for 24 hours. This was done 7 to 12 days after the organoids were split, seeded, and treated with differentiation medium to induce flat cell growth. To assess the apoptosis and lipid accumulation the researchers used caspase 3/7 detecting green fluorescence, red LipidTox, and the nuclear stain, Hoechst (McCarron et al., 2021).

This study was successful in using small amounts of liver from patients with MASH to create bipotent ductal organoids. It found that no sample failed to give stem cells and that a sample as small as 100 mg was sufficient to yield stem cells. The ideal range was 300-500 mg with the 100 mg showing a corresponding decrease in initial yield, but the morphology and growth remained the same. These MASH organoids exhibited a decreased ability to reach mature size and density, taking 2 weeks longer than the control to develop. A portion of the organoids had an irregular shape morphology while the others were spherical. The MASH organoids also had a limited capacity of expansion and division, slowing down and stopping after passages 8-16, whereas the controls expanded until passage 19 (McCarron et al., 2021).

Transcriptomics of the MASH liver-derived organoids revealed that many pathogenic pathways were upregulated and many cell cycle-related and growth-related pathways were downregulated. MASH individuals had diverse transcriptomics with no observable patterns compared to healthy individuals whose clusters all grouped together. Fibrosis markers and fibrosis-associated proteins were upregulated in end-stage MASH. These include the Aldo-keto reductase family 1 member B10 (AKR1B10), ubiquitin D

(UBD), cyclin D2 (CCND2), collagen type VI alpha 2 chain (COL6A2), dickkopf-related protein 3 (DDK3), and peroxidasin (PXDN) (McCarron et al., 2021).

Not only were the genetic profiles of the organoids altered from normal and similar to MASH patients, but their functionality also resembled MASH patients as well. The cytochrome p450 system involved in the metabolism of xenobiotics, steroid hormone synthesis, retinol metabolism, and bile acid synthesis was upregulated in a patient specific way. These MASH organoids also exhibited a reduction in albumin secretion which is in line with the decreased production of albumin in MASH livers. CYP3A4 activity was high, and ammonia degradation was highly variable. They showed a marked increase in sensitivity to apoptotic stimuli such as PA. The organoids also were proven to increase their FFA-induced lipid accumulation when exposed to oleic acid (McCarron et al., 2021). This study showed promise that organoids can be used to create personalized treatment for patients with MASH. Advancements such as improving procurement and combining these MASH patient-derived organoids with other cell types of the liver aid in their potential to screen for drugs and act as personalized treatment.

Wang et al. used an Organoids-on-a-Chip system from human-induced pluripotent stem cells (hiPSCs) to model MASLD. Organ chip technology provide a physiologically relevant microenvironment that maximized stem cell organoid potential. The study examined the heterogenous cellular morphology of the liver and its specific functions to ensure the 3D culture device accurately represented liver tissue. To do so, the liver Organoids-on-a-Chip were fabricated with poly(dimethylsiloxane) using lithography to have two layers with a micropillar array structure to reduce variability of organoid size.

The bottom layer allowed for cell aggregation, 3D culture and liver organoid generation while the top layer acted as a medium chamber for cell injection and fluid flow. The medium chamber allowed for perfusion and therefore nutrient exchange, waste exclusion, and external manipulation with FFAs.

The liver organoids were formed from hiPSCs cultured in mTeSR1 medium that was changed daily. To ensure their health and continued progression the organoids were digested with Accutase and passaged when they reached 70-90% confluency. The study employed a four-stage differentiation protocol to induce iPSCs to form a hepatic progenitor and eventually a mature liver morphology. Endoderm differentiation was achieved using RPMI-1640 medium with GlutaMAX, 1% KSR, B27, and activin-A on days 0-5. To aid with hepatic endoderm differentiation bFGF and BMP4 were added on days 5-8. It was clear that differentiation of this stage was successful as they endoderm established a typical flat and elongated shape. For hepatic progenitor differentiation and expansion, HGF was added on days 8-13. The progenitors were seen to exhibit a normal polygonal morphology. On day 10, the progenitors were digested with Accutase, resuspended in differentiation medium, and seeded on the micropillar chip allowing 3D aggregation to occur via overnight self-assembly. On day 13 the spheroids were placed in hepatocyte culture medium with oncostatin M and dexamethasone which facilitated hepatocyte differentiation and organoid formation. On day 18 the organoids were cultured without oncostatin M (Wang et al., 2020). An overview of the differentiation process and organoid-on-a-chip formation is summarized in figure 11. Once the organoids-on-a-chip were formed they were ready to model MASLD.

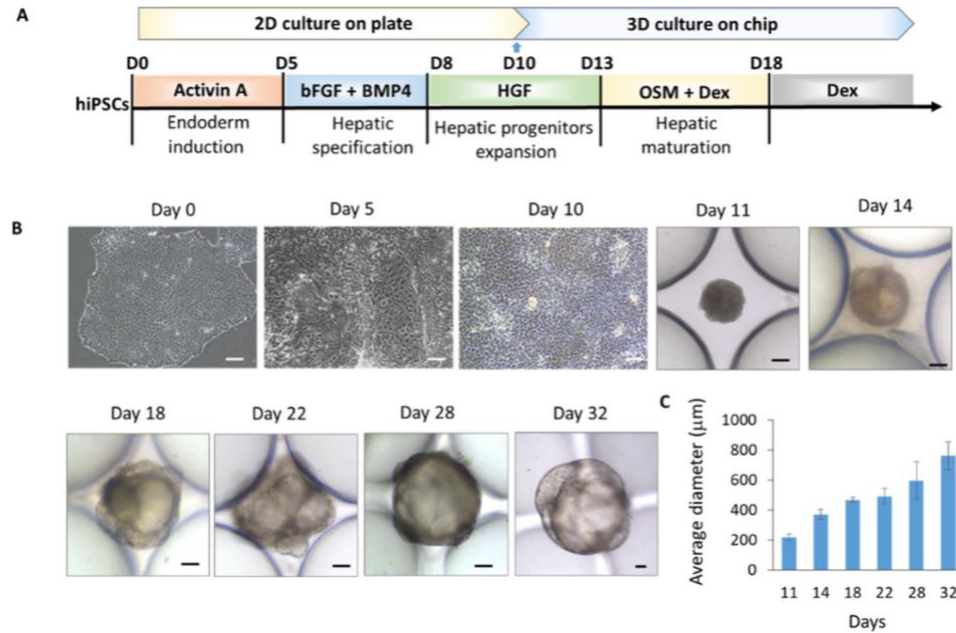


**Figure 11:** The process of forming 3D liver organoids on a chip through hiPSC differentiation. (A) Diagram of the protocol to differentiate hi-PSC-derived liver organoid. (B) the 2D cells and spheroids in 3D at different stages during development. (C) Organoid size distribution (Wang et al., 2020).

Upon confirmation that the liver organoid generation was successful, they were exposed to a continuous flow of 600  $\mu\text{M}$  FFAs for 7 days at day 23 of culture. The FFAs included a mixture of OA and PA at a 2:1 ratio conjugated to fatty acid-free BSA. The liver organoids were fixed, cut, and stained with primary and secondary antibodies, and DAPI to evaluate the effect of the FFAs. SYBR green RT-PCR using  $\beta$ -actin as the reference gene was performed. Oil Red O staining was used on cryosections of the organoids and imaged using a fluorescent microscope to assess lipid droplet formation. A TG accumulation kit was also used to confirm lipid droplet formation. To assess functionality of the organoids after their treatment with FFAs the supernatant was collected and using an ELISA kit the albumin secretion was measured. Cytotoxicity and intracellular ROS levels were measured using specific kits (Wang et al., 2020).

The continuous flow of FFAs successfully caused lipid droplets and TGs to accumulate after only 7 days of treatment. TG accumulation was also seen to gradually increase during prolonged FFA induction. Lipid metabolism-related genes were highly expressed such as APOC2, CPT2, CPT1A, and HADH. APOC2 (apolipoprotein C-II) serves as a lipid-binding protein necessary for lipid metabolism. The other three genes are related to fatty acid catabolism by the mitochondrial fatty acid  $\beta$ -oxidation pathway. The protein perilipin 2 which plays a role in lipid droplet formation and accumulation was widely expressed. ROS production was seen along with an elevation in the presence chronic inflammatory cytokines such as IL-6, IL-17, IL-8, and TNF- $\alpha$ . There was a marked increase in the LDH released into the media suggested an increase in cytotoxicity. An increase in the deposition of fibrogenic markers such as  $\alpha$ -SMA and an upregulation of COL1 showed evidence of fibrosis development (Wang et al., 2020). These changes in gene expression, morphology, and functionality contribute to the establishment that these liver-organoid-on-a-chip systems were successful in recapitulating key features of MASLD.

Pedersen et al. created dietary models for MASH in Göttingen Minipigs using three different diets. The diets were a high fat, fructose, and cholesterol (FFC) one and a choline-deficient, amino acid-defined high-fat diet (CDAHFD) either with sucrose (CDAHFD-S) or with the fructose (CDAHFD-F). The CDAHFD diet contained 1% cholesterol, 0.35% cholic acid, 30% fat (derived from milk fat and cocoa butter), no choline, 0.1% methionine. The CDAHFD-S contained 20% sucrose, and the CDAHFD-F contained 20% fructose. The pigs were fed their respective diet for 8 weeks. The FFC

pigs gained and the CDAHFD-S and CDAHFD-F lost weight. The relative weight of each group's liver increased with the CDAHFD groups showing the most increase (Pedersen et al., 2020). These diets were chosen for their resemblance to diets consumed by patients at risk for progressive MASLD development and because of their lipotoxic potentials.

Certain features of MASH were successfully recapitulated in the CDAHFD pigs such as steatosis, inflammation, and fibrosis. Macrovesicular steatosis was seen as early as two weeks of diet administration and worsened by week 8. TG and cholesterol levels were high as well in these groups. The CDAHFD groups and the FFC groups exhibited inflammatory cell infiltration but in the CDAHFD groups the inflammatory cells formed a crown-like structure around the hepatocytes, which is a specific feature of MASH. Infiltration was seen at 2 weeks and evidence of foamy macrophages that attempted to dissolve lipids were detected at 8 weeks. HSC activation and an increase in profibrotic gene expression in CDAHFD was evidence of a mild fibrotic response. Fibrosis wasn't detected at the 2-week marker, but early HSC activation was detected via  $\alpha$ -SMA presence. At week 8, fibrosis resembling chicken-wire was seen around the hepatocytes. Gene expression analysis was used to further validate that the diets induced a MASH response. There was an upregulation of inflammatory genes, lipid metabolism genes, and fibrosis-related genes in CDAHFD pigs. The inflammatory genes were CCL2, IL-6, CD-68, and TNF- $\alpha$ . The lipid metabolism genes that were altered and led to an increase in lipid uptake and transport were FABP4, CD-36, and LPL (Pedersen et al., 2020). Overall,

this study successfully modeled MASH and its various features in Göttingen Minipigs using a CDAHFD diet.

Charlton et al. established a small animal model of MASH using a diet that mimics the Western diet which is full of fast-food options. The high-fat and high-sugar diets were tested for their ability to induce metabolic dysfunction, hepatic steatosis, inflammation, and fibrosis. The study used both male and female C57BL/6J mice, a strain of mice found to be more susceptible to disease progression and therefore is commonly used for metabolic disease research. There were three different diets fed to the mice: 1) a standard chow (SC) with 13% energy from fat and 1% saturated fat; 2) High-Fat (HF) Diet with 60% energy from fat and 1% saturated fat; and 3) Fast food (FF) diet with 40% energy from fat, 12% saturated fat and 2% cholesterol with high fructose supplementation (Charlton et al., 2011).

Overall, the HF and FF diets induced obesity and caused IR. The FF diet, specifically, caused ballooning of hepatocytes and progressive fibrosis. The histology of the livers from each group was assessed and is shown in figure 12. The SC group, the control group, showed normal histology. The HF diet group exhibited mild steatosis but no inflammation or fibrosis. The FF diet was most successful at closely recapitulating human MASH features. The histology showed pronounced steatohepatitis, hepatocyte ballooning, and stage 2 fibrosis. Picosirius Red staining was used to assess collagen accumulation and Masson's trichrome staining was used to assess fibrotic tissue formation and perisinusoidal/pericellular fibrosis. The gene expression of ER stress markers, a lipoapoptosis marker, markers of oxidative stress and DNA damage, apoptosis

markers, and fibrosis markers was analyzed. The FF diet showed a marked upregulation in ER stress markers such as PERK, CHOP, and ATF6. Lipoapoptosis marker levels, specifically PUMA a pro-apoptotic protein in mitochondrial cell death pathways, were similar across both the HF and FF diets. SOD1, a marker that protects against oxidative damage, was also similar between the groups. An indicator of oxidative DNA damage, 8-hydroxydeoxyguanosine, that is induced by oxidative radicals was similar among all groups as well. Apoptosis markers were found to be elevated using TdT dUTP nick end labeling of DNA strand breaks with fluorescein. Some fibrosis markers that were upregulated in FF were TGF- $\beta$ 1 (5-fold increase), COL1A1 (17-fold increase), and TIMP1. These results all showed that the FF group had increased fibrosis, inflammation, and ER stress which was linked to lipotoxicity and liver damage elicited by the diet they were fed (Charlton et al., 2011). The FF model was the most successful in recapitulating MASH features giving it the potential to aid in translation preclinical studies and drug testing.

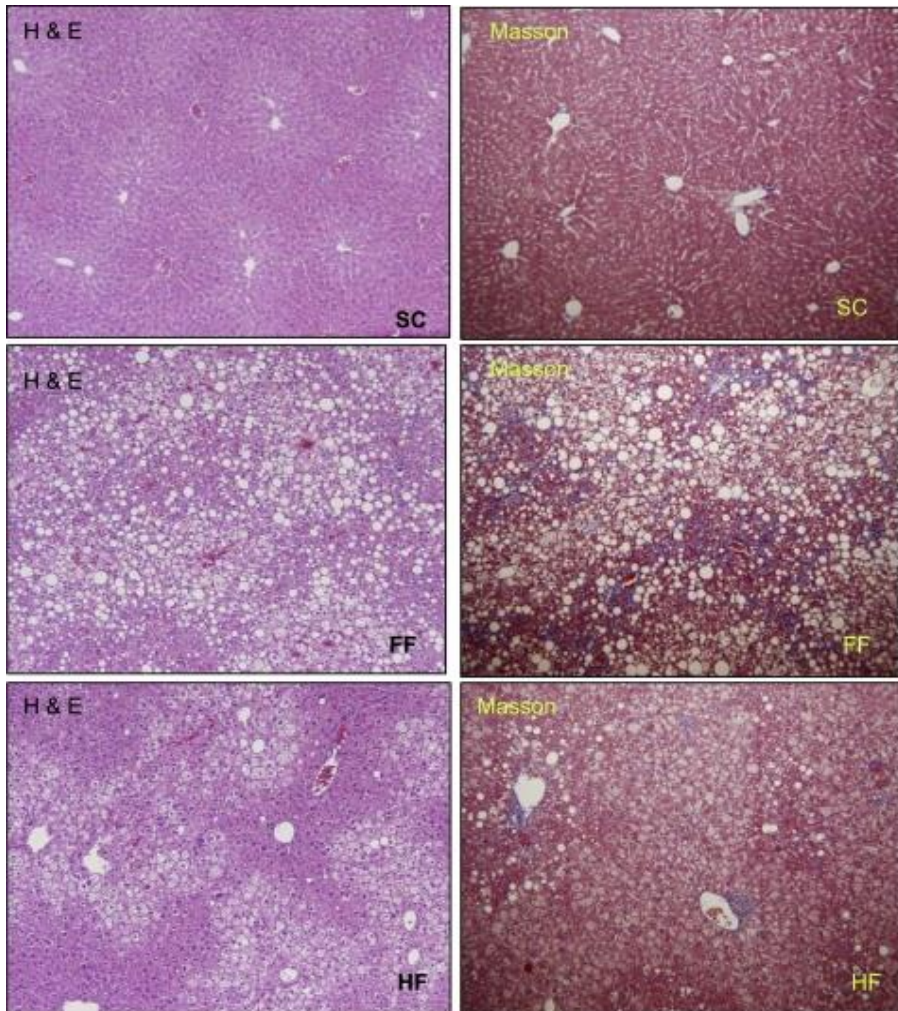


**Figure 12:** H&E staining of SC, FF, and HF diet fed mice on the left and Masson's Trichrome of each diet on the right (Charlton et al., 2011).

Ströbel et al. created a complex 3D human in vitro model using human liver microtissues (hLiMTs) that contain PHHs, liver endothelial cells (LECs, also known as LSECs), Kupffer cells (KCs), and HSCs. This model contains all the relevant liver cells that play a major role in the development of MASH in MASLD patients. Control hLiMTs were exposed to lean conditions that involved culture in basal hepatocyte maintenance medium to induce MASH features, the hLiMTs were exposed to a MASH media that contained elevated glucose and fructose levels (total of 22.5 mM), FFAs at 167  $\mu$ M, and

LPS at 5  $\mu\text{g}/\text{mL}$ . Medium was changed on days 0, 3, 5, and 7. The specific FFAs used were the unsaturated acid, oleic acid, and the saturated acid, palmitic acid. Various endpoint assays were performed to assess the effect of the acids on the liver microtissues. LDH that is measured in the supernatant following release from damaged cells using the LDH-Glo Cytotoxicity Assay kit. Intracellular TG content was measured using a kit after the hLiMTs were washed with PBS, lysed, and incubated for 1 hour. Procollagen I level in the supernatants collected on days 7 and 10 were measured to evaluate the progression of fibrosis. Immunohistochemistry staining was used to investigate the presence of a fibrotic environment. Inflammatory pathway activation was calculated by measuring the secretion of various cytokines such as IL-6, IP-10, IL-8, MCP-1, MIP-1, TNF- $\alpha$ , and MIP-1 $\alpha$ . On day 10 of treatment, Nile red and DAPI staining was performed after washing the hLiMTs with PBS to assess for lipid accumulation. RNA sequencing was performed and analyzed to discover the gene expression profiles of the microtissues (Ströbel et al., 2021).

It was first confirmed that the 3D liver microtissues retained their cellular components of PHHs, LECs, HSCs, and KCs after the 10 days of treatment. The MASH treatment was not found to be cytotoxic to the microtissues and all their cells remained viable and intact. The treatment was effective at increasing intracellular lipid content and TG levels which was evident with Nile Red staining. Displaced nuclei seen on imaging suggested there was hepatocyte ballooning, a key MASH feature. The upregulation of the inflammatory cytokines mentioned above compared to the lean treatment group showed that the MASH treatment results in inflammation. A fibrotic phenotype was effectively

induced by the MASH media. IHC showed that MASH hLiMTs expressed a higher protein levels of collagen type I and III compared to the lean media. A product of procollagen I synthesis was found in the supernatant of the MASH microtissues suggesting that there was active fibrosis development via collagen synthesis. Sirius Red staining of histological sections showed the presence of collagen fibrillation consistent with pathological changes seen in MASH patients. Whole transcriptomic profiles were taken on days 5 and 10 and the sample's distinct clustering indicated there was divergent phenotypes in the MASH group. Lipid metabolism genes such as FASN, CYP3A4, and PPARA were found to be downregulated suggesting there was metabolic dysregulation in the MASH group. Fibrosis markers such as COL1A2, TIMP1, and FN1 were upregulated providing further evidence that fibrosis was initiated (Ströbel et al., 2021). This study accurately mimicked clinical MASH features and provided a potential platform for clinical drug testing to treat patients.

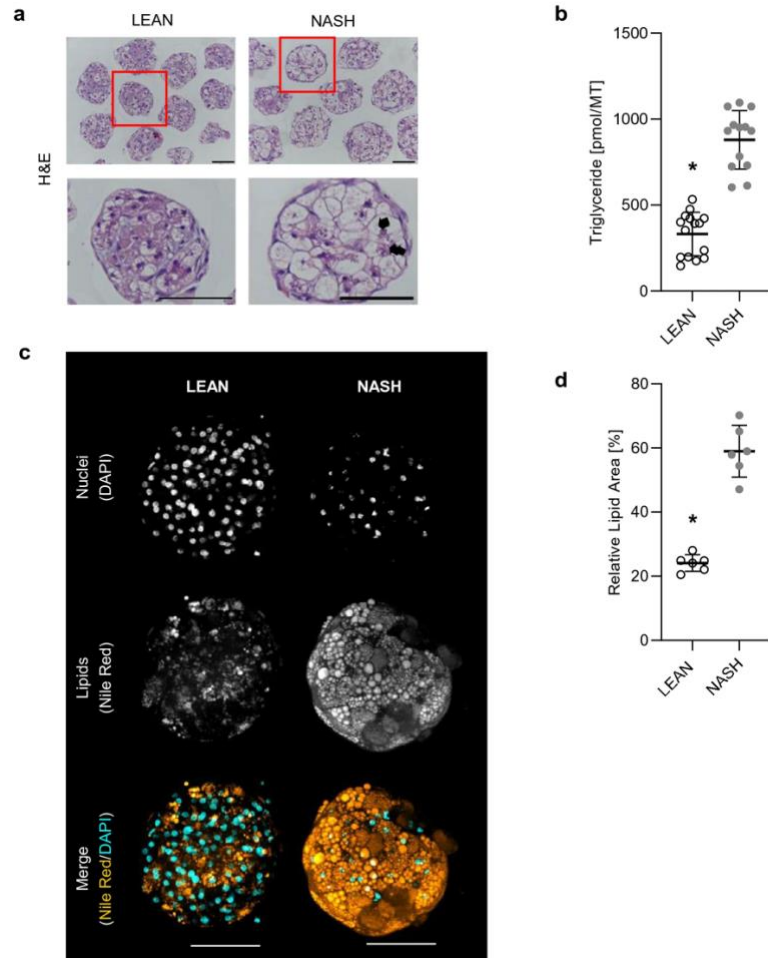


**Figure 13:** MASH-treated hLiMTs exhibited steatosis-like phenotype and lipid accumulation. (a) H&E staining that exhibits an accumulation of lipids in MASH hLiMTs compared to Lean control. Hepatocyte ballooning is depicted by the arrows. (b) Steatosis-like phenotype was confirmed in MASH hLiMTs with an increase in TG levels. (c) Nile Red staining shows an increase in intracellular lipids in the MASH hLiMTs seen as both small and large lipids droplets. (d) Significant increase in lipids found in MASH hLiMTs evident by high content image-based quantification of lipid content. (Ströbel et al., 2021).

## DISCUSSION

Despite MASLD's increasing prevalence and poor patient outcomes there is not an FDA-approved medication or treatment for this disease. This notion has caused many researchers to dedicate their studies to modeling the disease in vitro and in vivo in an attempt to create a platform to understand the pathophysiology of these disease and potential therapeutic targets. Unfortunately, there has been limited success in the production of a wide-range model that faithfully recapitulates the disease and allows this testing. The various models examined in this thesis include in vivo animal models using mice and minipigs and 3D in vitro models using primary derived tissue, hiPSC-derived organoids, organoids-on-a-chip, and liver microtissues. The next step is to understand why many of these models fall short in their goal and to determine future actions for this field to take in order to attain the ultimate goal of treating this complex disease.

Various studies have explained and agreed that the use of 2D cell culture methods is not sufficient to model this disease. A 2D monolayer cell culture system, although cheap, easy to handle, and compatible with high-throughput applications, does not provide the necessary interplay between each cell type of the liver that occurs during MASLD and MASH. These models only contain singular hepatic cell types and therefore lack the vital non-parenchymal cells involved in this disease. The absence of proinflammatory and profibrotic cell types makes this model not suitable to depict MASL to MASH progression (Han et al., 2023). 2D culture of single hepatic cell types are also seen to lose liver-specific functionality within days of culture making them unsuitable for repeated dosing and long-term studies (Mukherjee et al., 2019). The many limitations of

2D models are essentially why there was not a specific model discussed in this thesis, but it is still important to understand why alternative methods were devised.

Diet-induced animal models, such as the ones previously discussed, can more closely resemble disease heterogeneity and cellular crosstalk since they have the cells and other involved organs present. Animal models, however, still have great limitations that require other methods to be explored. For example, there are many genetic discrepancies and little overlap between humans and animals that impede the translation of findings from an animal model to clinical applications (Han et al., 2023; McCarron et al., 2021). There are also physiological differences between humans and animals that may cause the animals to present the spectrum of the disease differently or to metabolize diets and drugs differently. The specific outcome of the models are variable depending on the strain, species, and gender of the animal (Han et al., 2023; Ramli et al., 2020; Wang et al., 2020). The study conducted by Pedersen using minipigs was evidence of these limitations. Although they were able to show steatosis, TG level increase, fibrosis, and an inflammatory response, this model lacked the development of IR and obesity which are two important risk and driving factors of the disease (Pedersen et al., 2020). The study conducted by Elbadawy et al. used diet induced mouse MASH livers to develop organoids that model the different levels of MASH severity. This model not only complicated its ability to translate to humans by adding two dissimilar variables rather than one, but similarly to Pedersen et al. they found there was a lack of important features in their model. Once transferred from the in vivo model to the in vitro model, activated HSCs were found to not survive as the culture system was not suitable for them. HSCs

are an important factor in MASH development, maintenance, and progression therefore making their absence detrimental to the model (Elbadawy et al., 2020). Another limitation found in these studies is the long period of time required to induce advanced disease progression in animal models. Charlton et al. showed that mice needed to be fed the “fast food” diet for 6 months to induce advanced levels of fibrosis and Pedersen et al. concluded 8 weeks was not long enough to induce advanced fibrosis in minipigs (Charlton et al., 2011; Pedersen et al., 2020). These significantly long periods of feeding make animal models non-ideal because they are limited in their ability to produce results in a timely manner. Combining the period of feeding, downstream analysis, revising experimental methods, and conducting another study, the timeline of these animal models to produce contributions to the field is unrealistic.

The limitations of 2D and animal models to recapitulate MASLD requires the production of more advanced 3D in vitro modeling. 3D in vitro modeling can avoid the lack of crosstalk and species-specific differences seen in 2D and animal models. It has a heightened similarity of the complex liver structure and phenotype. 3D models are capable of metabolic activity and functionality that closely resembles that of the human physiology. These models are also more robust and stable in culture than their 2D counterparts. Microtissues such as the 3D-hLMT's in Mukherjee et al.'s study and the hLiMTs in Ströbel et al.'s study are an example of a 3D model shown to overcome the many limitations of animal and 2D models. They are composed of liver specific cells that are in proportions that resemble that of the native liver. In both studies there was no detectable necrosis or loss of viability showing they are stable in long-term studies. The

microtissues are capable of existing and creating a liver specific microenvironment. These models were rather successful in resembling the physiology of MASLD in accumulating lipids, developing fibrosis, and exhibiting apoptosis. Mukherjee et al. and Ströbel et al., although exhibiting some MASLD features, had limitations, suggesting that adjustments and the investigation of another 3D modeling type may be necessary. They both lacked the recruitment of circulating cells and peripheral immune cell infiltration. These cells are crucial in later stages of MASH progression and without them testing disease reversal mechanisms is restricted. The microtissues in both showed a limited capacity to model advanced fibrotic stages and a need to devise quantification methods that are more closely associated with clinical diagnostic markers. 3D microtissues also create an issue of modeling drug and treatment effects as the interplay with other organs is not able to be replicated in these systems (Han et al., 2023; Mukherjee et al., 2019; Ströbel et al., 2021). Again, although microtissues are a promising model for MASLD and MASH features, their limitations suggest that a new 3D model is needed. This model should closely mimic the complex environment of not only the liver but also the many other organs involved. It should be able to resemble not only the early stages of this disease but also the more advanced ones. A new model must account for the limitations seen currently in these.

Han et al. is a review that specifically discusses the benefits of using 3D multicellular aggregates (organoids) to model MASLD rather than the methods currently employed, providing a nice overview of the previous discussion. 2D cell culture using only hepatocyte-like cells, as mentioned, has its limitations, found in their reduced

function and limited proliferative potential. The monocellular nature of a 2D model also causes it to lack pro-fibrotic and pro-inflammatory cell types not allowing the model to fully recapitulate the heterogenous nature of the cellular environment of the liver. The use of primary human hepatocytes is limited because their restricted accessibility and rapid loss of function. Animal models, although successful at modeling the disease progression of MASLD, differ too greatly in their genetic and physiological profile making translation of findings to humans extremely difficult. The solution to fix all these limitations is 3D liver organoids which have an accurate structure capable of functioning properly and expanding throughout culture. Multicellular liver organoids with parenchymal and non-parenchymal cells are even capable of forming a fully functioning bile canaliculi network (Han et al., 2023). Ramli et al. further explains how organoid models can mimic the cellular complexity and interactions between cells since the cells aggregate and communicate together. They are capable of accurately replicating MASLD and MASH proven by their exhibition of structural and metabolic changes after exposure to FFAs which are seen in human cases. Depending on the process of development, i.e. if patient-specific cells are used, organoid systems even have the potential for personalized medicine tailored specifically to the patient's disease profile (Ramli et al., 2020). The main issue, however, with multi-cellular 3D organoids is there are several different differentiation protocols the ultimately lead to diverse variances between organoids (Han et al., 2023).

This thesis discussed many modeling techniques and found they often fall short of truly representing the disease features of MASLD. Therefore, a new proposal will now be

suggested that is a culmination of all the best parts of the previously discussed models. When designing an organoid model care must be taken when choosing the cell types one is going to use. The many studies this thesis discussed employ different cell types that act as the hepatocyte component of the liver such as HepaRG cells, primary hepatocytes from mice or humans, and hiPSC-induced hepatocyte-like cells. As discussed, primary hepatocytes rapidly lose their functionality and are quite arduous and expensive to obtain. Gwag et al., Elbadawy et al., and McCarron et al. all used hepatocytes from primary liver tissues making their models susceptible to these limitations. Elbadawy et al., specifically used primary liver disease obtained from mice which makes this model vulnerable to the limitations of animal models such as lacking genetic alignment. Although there was varying success from these models in recapitulating the features of MASLD and MASH, it is necessary to consider whether employing a more robust cell type would further improve the model's ability to faithfully encompass all disease features (Elbadawy et al., 2020; Gwag et al., 2022; McCarron et al., 2021). hiPSC-derived hepatocyte-like cells were used in Han et al.'s study and Wang et al.'s study. Before establishing the organoids these hiPSCs underwent a series of highly regulated differentiation protocols induced by growth factors. These cells once hepatocyte-like only possessed immature hepatic function, a low expression of CYP enzymes, and an immature phenotype. They were capable of modeling MASH and MASLD but only to a small degree with minor lipid accumulation (Gwag et al., 2022; Han et al., 2023). Another potential downfall of this cell type is they lack the defined epigenetic features seen normal or diseased livers and as explained previously, epigenetic modifications play an important role in disease risk and

development. Hepatocyte-like cells from hiPSCs also are prone to develop spontaneous mutations at a faster rate than other cell types (McCarron et al., 2021). The cell type employed by Bronsard et al., the HepaRG cell line has proven to be the optimal choice in modeling metabolic disorders and diseases such as MASLD. They closely resemble primary human hepatocytes, are capable of albumin production, and xenobiotic metabolism. Upon treatment with specific culture media, these cells can differentiate into hepatocyte-like and cholangiocyte-like cells. This study showed they are capable of accumulating lipids when exposed to FFAs, therefore mimicking steatosis seen in MASLD. They also, upon co-culture with LX-2 cells and macrophages were found to successfully model the fibrosis and inflammation seen in later stages of the disease, specifically MASH (Bronsard et al., 2024). These benefits and the results of Bronsard et al. suggest HepaRG cells to be the most optimal choice when creating an organoid model. It is also important to co-culture these cells with relevant liver cell types important for modeling the disease such as HSCs, LSEC, and Kupffer cells.

The next step in curating an organoid modeling system for MASLD is determining the concentration and identity of free fatty acids used to induce the disease as well as the timeline for treatment. The studies discussed employed different ratios of fatty acid mixtures at varying time points depending on the desired effect. Oleic acid and palmitic acid are traditionally used in MASLD models as these are the two fatty acids found the most in human patients. Palmitic acid is known to have more hepatotoxic effects and induce a more severe phenotype, especially one involving fibrosis. In order to model the progressive nature of the disease, it may be beneficial to alter the FFA treatment

increasing the concentration of FFAs delivered to the organoids as well as increasing the amount of PA. To model steatosis, 300-500  $\mu\text{M}$  of oleic acid and palmitic acid at a 2:1 ratio conjugated to fatty acid-free BSA should be administered to the fully differentiated liver organoids. This treatment should last 48 hours with media being changed and readministered at 24 hours. It is important to remember that steatosis is simply lipid accumulation from an excess of FFA exposure. Organoids and supernatants should be collected at both the 24 and 48 hours timepoints to assess the degree of lipid accumulation and to ensure that no fibrosis, inflammation, or necrosis were induced by this concentration or duration of FFA exposure. To model the next step in disease progression, MASH, the ratio of FFAs should be switched to involve a higher concentration of palmitic acid than oleic acid and treatment should be longer. The MASH inducing media in Gwag et al. had promising effects in inducing a MASH phenotype. It contained PA, high glucose, and LPS all of which are seen to induce an increase in inflammation and fibrosis, both of which are necessary to model MASH. Another option would be to increase the concentration to above 500  $\mu\text{M}$  FFAs with a 1:2 ratio of oleic to palmitic acid. This treatment should be given between 5-10 days with organoids being pulled on days 5 and 10 to determine the optimal exposure. Finally, next in the progression of MASLD is developing severe fibrosis with the potential of leading to cirrhosis and possibly liver failure. A severe fibrotic phenotype was investigated by Mukherjee et al. solely using palmitic acid administered for a 9-day period. The robust induction of liver injury and apoptosis shown by this model makes it promising to test again in modeling the progression of MASLD.

Overall, a combination of modeling techniques from the organoid studies investigated is proposed in an attempt to combat the shortcomings and gaps in MASLD modeling. An organoid model using HepaRG cells, LSEC, HSCs (LX-2), and Kupffer cells will closely recapitulate the human liver's phenotype, functioning, and complex cell-to-cell interactions. Starting with a low dose of palmitic acid compared to oleic acid for a short period of time is necessary to induce simple steatosis only. To model the progression from simple steatosis to MASH the ratio of FFAs should favor palmitic acid and exposure should be increased to approximately 9 days. The treatment should then be switched solely to palmitic acid administration for at least 5 more days to induce severe fibrosis.

## CONCLUSION

MASLD presents challenges when attempting to model the complexity involved in its cell-to-cell communications, development, and progression. Despite these challenges, it is crucial to create a modeling system capable of recapitulating all the features of this disease. This model can then aid in bridging the gap between diagnosis and treatment seen in clinics. The use of 3D organoid in vitro techniques provides a promising platform for doing just that. This technique, however, still must undergo vigorous testing to ensure it is capable of consistently producing a system that not only faithfully models the environment of the liver but also accurately depicts the features of the stages of MASLD. This thesis simply provided a framework to explain there was a need and attempted at fixing the need. There is still a need for a standardized protocol to form these organoids and to induce MASLD within them so they can be used for downstream, therapeutic analysis.

**BIBLIOGRAPHY**

- Ayonrinde, O. T., Olynyk, J. K., Beilin, L. J., Mori, T. A., Pennell, C. E., de Klerk, N., Oddy, W. H., Shipman, P., & Adams, L. A. (2011). Gender-Specific Differences in Adipose Distribution and Adipocytokines Influence Adolescent Nonalcoholic Fatty Liver Disease. *Hepatology*, *53*(3), 800. <https://doi.org/10.1002/hep.24097>
- Bence, K. K., & Birnbaum, M. J. (2021). Metabolic drivers of non-alcoholic fatty liver disease. *Molecular Metabolism*, *50*, 101143. <https://doi.org/10.1016/j.molmet.2020.101143>
- Boursier, J., Mueller, O., Barret, M., Machado, M., Fizanne, L., Araujo-Perez, F., Guy, C. D., Seed, P. C., Rawls, J. F., David, L. A., Hunault, G., Oberti, F., Calès, P., & Diehl, A. M. (2016). The severity of nonalcoholic fatty liver disease is associated with gut dysbiosis and shift in the metabolic function of the gut microbiota. *Hepatology*, *63*(3), 764. <https://doi.org/10.1002/hep.28356>
- Bronsard, J., Savary, C., Massart, J., Viel, R., Moutaux, L., Catheline, D., Rioux, V., Clement, B., Corlu, A., Fromenty, B., & Ferron, P. J. (2024). 3D multi-cell-type liver organoids: A new model of non-alcoholic fatty liver disease for drug safety assessments. *Toxicology in Vitro*, *94*, 105728. <https://doi.org/10.1016/j.tiv.2023.105728>
- Bujanda, L., Hijona, E., Larzabal, M., Beraza, M., Aldazabal, P., García-Urkiá, N., Sarasqueta, C., Cosme, A., Irastorza, B., González, A., & Arenas, J. I. (2008). Resveratrol inhibits nonalcoholic fatty liver disease in rats. *BMC Gastroenterology*, *8*(1), 40. <https://doi.org/10.1186/1471-230X-8-40>

- Carr, R. M., Oranu, A., & Khungar, V. (2016). Nonalcoholic Fatty Liver Disease: Pathophysiology and Management. *Gastroenterology Clinics of North America*, 45(4), 639–652. <https://doi.org/10.1016/j.gtc.2016.07.003>
- Charlton, M., Krishnan, A., Viker, K., Sanderson, S., Cazanave, S., McConico, A., Masuoko, H., & Gores, G. (2011). Fast food diet mouse: Novel small animal model of NASH with ballooning, progressive fibrosis, and high physiological fidelity to the human condition. *American Journal of Physiology - Gastrointestinal and Liver Physiology*, 301(5), G825–G834. <https://doi.org/10.1152/ajpgi.00145.2011>
- Clemens, D. L. (2006). Use of Cultured Cells to Study Alcohol Metabolism. *Alcohol Research & Health*, 29(4), 291–295.
- Delli Bovi, A. P., Marciano, F., Mandato, C., Siano, M. A., Savoia, M., & Vajro, P. (2021). Oxidative Stress in Non-alcoholic Fatty Liver Disease. An Updated Mini Review. *Frontiers in Medicine*, 8. <https://doi.org/10.3389/fmed.2021.595371>
- Ding, S., Jiang, J., Zhang, G., Bu, Y., Zhang, G., & Zhao, X. (2017). Resveratrol and caloric restriction prevent hepatic steatosis by regulating SIRT1-autophagy pathway and alleviating endoplasmic reticulum stress in high-fat diet-fed rats. *PLOS ONE*, 12(8), e0183541. <https://doi.org/10.1371/journal.pone.0183541>
- Ehrlich, L., Scrushy, M., Meng, F., Lairmore, T. C., Alpini, G., & Glaser, S. (2018). Biliary epithelium: A neuroendocrine compartment in cholestatic liver disease. *Clinics and Research in Hepatology and Gastroenterology*, 42(4), 296–305. <https://doi.org/10.1016/j.clinre.2018.03.009>

- Elbadawy, M., Yamanaka, M., Goto, Y., Hayashi, K., Tsunedomi, R., Hazama, S., Nagano, H., Yoshida, T., Shibutani, M., Ichikawa, R., Nakahara, J., Omatsu, T., Mizutani, T., Katayama, Y., Shinohara, Y., Abugomaa, A., Kaneda, M., Yamawaki, H., Usui, T., & Sasaki, K. (2020). Efficacy of primary liver organoid culture from different stages of non-alcoholic steatohepatitis (NASH) mouse model. *Biomaterials*, 237, 119823. <https://doi.org/10.1016/j.biomaterials.2020.119823>
- Fracanzani, A. L., Valenti, L., Bugianesi, E., Andreoletti, M., Colli, A., Vanni, E., Bertelli, C., Fatta, E., Bignamini, D., Marchesini, G., & Fargion, S. (2008). Risk of severe liver disease in nonalcoholic fatty liver disease with normal aminotransferase levels: A role for insulin resistance and diabetes. *Hepatology (Baltimore, Md.)*, 48(3), 792–798. <https://doi.org/10.1002/hep.22429>
- Gangarapu, V., Ince, A. T., Baysal, B., Kayar, Y., Kiliç, U., Gök, Ö., Uysal, Ö., & Senturk, H. (2015). Efficacy of rifaximin on circulating endotoxins and cytokines in patients with nonalcoholic fatty liver disease. *European Journal of Gastroenterology & Hepatology*, 27(7), 840. <https://doi.org/10.1097/MEG.0000000000000348>
- Gerges, S. H., Wahdan, S. A., Elsherbiny, D. A., & El-Demerdash, E. (2021). Non-alcoholic fatty liver disease: An overview of risk factors, pathophysiological mechanisms, diagnostic procedures, and therapeutic interventions. *Life Sciences*, 271, 119220. <https://doi.org/10.1016/j.lfs.2021.119220>

- Gwag, T., Ma, E., Zhou, C., & Wang, S. (2022). Anti-CD47 antibody treatment attenuates liver inflammation and fibrosis in experimental non-alcoholic steatohepatitis models. *Liver International : Official Journal of the International Association for the Study of the Liver*, 42(4), 829–841.  
<https://doi.org/10.1111/liv.15182>
- Han, D. W., Xu, K., Jin, Z.-L., Xu, Y.-N., Li, Y.-H., Wang, L., Cao, Q., Kim, K.-P., Ryu, D., Hong, K., & Kim, N.-H. (2023). Customized liver organoids as an advanced in vitro modeling and drug discovery platform for non-alcoholic fatty liver diseases. *International Journal of Biological Sciences*, 19(11), 3595–3613.  
<https://doi.org/10.7150/ijbs.85145>
- Harrison, S. A., Bedossa, P., Guy, C. D., Schattenberg, J. M., Loomba, R., Taub, R., Labriola, D., Moussa, S. E., Neff, G. W., Rinella, M. E., Anstee, Q. M., Abdelmalek, M. F., Younossi, Z., Baum, S. J., Francque, S., Charlton, M. R., Newsome, P. N., Lanthier, N., Schiefke, I., ... Ratziu, V. (2024). A Phase 3, Randomized, Controlled Trial of Resmetirom in NASH with Liver Fibrosis. *New England Journal of Medicine*, 390(6), 497–509.  
<https://doi.org/10.1056/NEJMoa2309000>
- Hora, S., & Wuestefeld, T. (2023). Liver Injury and Regeneration: Current Understanding, New Approaches, and Future Perspectives. *Cells*, 12(17), 2129.  
<https://doi.org/10.3390/cells12172129>
- Horie, T., Ono, K., Horiguchi, M., Nishi, H., Nakamura, T., Nagao, K., Kinoshita, M., Kuwabara, Y., Marusawa, H., Iwanaga, Y., Hasegawa, K., Yokode, M., Kimura,

- T., & Kita, T. (2010). MicroRNA-33 encoded by an intron of sterol regulatory element-binding protein 2 (Srebp2) regulates HDL in vivo. *Proceedings of the National Academy of Sciences*, *107*(40), 17321–17326.  
<https://doi.org/10.1073/pnas.1008499107>
- Huang, P. L. (2009). A comprehensive definition for metabolic syndrome. *Disease Models & Mechanisms*, *2*(5–6), 231–237. <https://doi.org/10.1242/dmm.001180>
- Juanola, O., Martínez-López, S., Francés, R., & Gómez-Hurtado, I. (2021). Non-Alcoholic Fatty Liver Disease: Metabolic, Genetic, Epigenetic and Environmental Risk Factors. *International Journal of Environmental Research and Public Health*, *18*(10), Article 10. <https://doi.org/10.3390/ijerph18105227>
- Kalra, A., Yetiskul, E., Wehrle, C. J., & Tuma, F. (2025). Physiology, Liver. In *StatPearls*. StatPearls Publishing.  
<http://www.ncbi.nlm.nih.gov/books/NBK535438/>
- Kammel, A., Saussenthaler, S., Jähnert, M., Jonas, W., Stirm, L., Hoeflich, A., Staiger, H., Fritsche, A., Häring, H.-U., Joost, H.-G., Schürmann, A., & Schwenk, R. W. (2016). Early hypermethylation of hepatic Igfbp2 results in its reduced expression preceding fatty liver in mice. *Human Molecular Genetics*, *25*(12), 2588–2599.  
<https://doi.org/10.1093/hmg/ddw121>
- Koek, G. H., Liedorp, P. R., & Bast, A. (2011). The role of oxidative stress in non-alcoholic steatohepatitis. *Clinica Chimica Acta*, *412*(15), 1297–1305.  
<https://doi.org/10.1016/j.cca.2011.04.013>

- Loomba, R., Seguritan, V., Li, W., Long, T., Klitgord, N., Bhatt, A., Dulai, P. S., Caussy, C., Bettencourt, R., Highlander, S. K., Jones, M. B., Sirlin, C. B., Schnabl, B., Brinkac, L., Schork, N., Chen, C.-H., Brenner, D. A., Biggs, W., Yooseph, S., ... Nelson, K. E. (2017). Gut Microbiome-Based Metagenomic Signature for Non-invasive Detection of Advanced Fibrosis in Human Nonalcoholic Fatty Liver Disease. *Cell Metabolism*, 25(5), 1054-1062.e5.  
<https://doi.org/10.1016/j.cmet.2017.04.001>
- Masuoka, H. C., & Chalasani, N. (2013). Nonalcoholic fatty liver disease: An emerging threat to obese and diabetic individuals. *Annals of the New York Academy of Sciences*, 1281(1), 106–122. <https://doi.org/10.1111/nyas.12016>
- McCarron, S., Bathon, B., Conlon, D. M., Abbey, D., Rader, D. J., Gawronski, K., Brown, C. D., Olthoff, K. M., Shaked, A., & Raabe, T. D. (2021). Functional Characterization of Organoids Derived From Irreversibly Damaged Liver of Patients With NASH. *Hepatology*, 74(4), 1825–1844.  
<https://doi.org/10.1002/hep.31857>
- McCullough, A. J. (2006). Pathophysiology of Nonalcoholic Steatohepatitis. *Journal of Clinical Gastroenterology*, 40, S17.  
<https://doi.org/10.1097/01.mcg.0000168645.86658.22>
- Mukherjee, S., Zhelnin, L., Sanfiz, A., Pan, J., Li, Z., Yarde, M., McCarty, J., & Jarai, G. (2019). Development and validation of an in vitro 3D model of NASH with severe fibrotic phenotype. *American Journal of Translational Research*, 11(3), 1531–1540.

- Mummadi, R. R., Kasturi, K. S., Chennareddygari, S., & Sood, G. K. (2008). Effect of Bariatric Surgery on Nonalcoholic Fatty Liver Disease: Systematic Review and Meta-Analysis. *Clinical Gastroenterology and Hepatology*, 6(12), 1396–1402. <https://doi.org/10.1016/j.cgh.2008.08.012>
- Newsome, P. N., Buchholtz, K., Cusi, K., Linder, M., Okanoue, T., Ratziu, V., Sanyal, A. J., Sejling, A.-S., & Harrison, S. A. (2021). A Placebo-Controlled Trial of Subcutaneous Semaglutide in Nonalcoholic Steatohepatitis. *New England Journal of Medicine*, 384(12), 1113–1124. <https://doi.org/10.1056/NEJMoa2028395>
- Nguyen, P., Leray, V., Diez, M., Serisier, S., Bloc'h, J. L., Siliart, B., & Dumon, H. (2008). Liver lipid metabolism. *Journal of Animal Physiology and Animal Nutrition*, 92(3), 272–283. <https://doi.org/10.1111/j.1439-0396.2007.00752.x>
- Ong, J. P., Elariny, H., Collantes, R., Younoszai, A., Chandhoke, V., Reines, H. D., Goodman, Z., & Younossi, Z. M. (2005). Predictors of Nonalcoholic Steatohepatitis and Advanced Fibrosis in Morbidly Obese Patients. *Obesity Surgery*, 15(3), 310–315. <https://doi.org/10.1381/0960892053576820>
- Papatheodoridis, G. V., Goulis, J., Christodoulou, D., Manolakopoulos, S., Raptopoulou, M., Andrioti, E., Alexandropoulos, N., Savvidou, S., Papachristou, A., Zervou, E., Seferiadis, K., Kousidou, P., Vogiatzakis, E., & Tsianos, E. (2007). High prevalence of elevated liver enzymes in blood donors: Associations with male gender and central adiposity. *European Journal of Gastroenterology & Hepatology*, 19(4), 281. <https://doi.org/10.1097/MEG.0b013e328011438b>

- Pedersen, H. D., Galsgaard, E. D., Christoffersen, B. Ø., Cirera, S., Holst, D., Fredholm, M., & Latta, M. (2020). NASH-inducing Diets in Göttingen Minipigs. *Journal of Clinical and Experimental Hepatology*, *10*(3), 211–221.  
<https://doi.org/10.1016/j.jceh.2019.09.004>
- Pouwels, S., Sakran, N., Graham, Y., Leal, A., Pintar, T., Yang, W., Kassir, R., Singhal, R., Mahawar, K., & Ramnarain, D. (2022). Non-alcoholic fatty liver disease (NAFLD): A review of pathophysiology, clinical management and effects of weight loss. *BMC Endocrine Disorders*, *22*(1), 63.  
<https://doi.org/10.1186/s12902-022-00980-1>
- Powell, E. E., Wong, V. W.-S., & Rinella, M. (2021). Non-alcoholic fatty liver disease. *The Lancet*, *397*(10290), 2212–2224. [https://doi.org/10.1016/S0140-6736\(20\)32511-3](https://doi.org/10.1016/S0140-6736(20)32511-3)
- Ramli, M. N. B., Lim, Y. S., Koe, C. T., Demircioglu, D., Tng, W., Gonzales, K. A. U., Tan, C. P., Szczerbinska, I., Liang, H., Soe, E. L., Lu, Z., Ariyachet, C., Yu, K. M., Koh, S. H., Yaw, L. P., Jumat, N. H. B., Lim, J. S. Y., Wright, G., Shabbir, A., ... Chan, Y.-S. (2020). Human Pluripotent Stem Cell-Derived Organoids as Models of Liver Disease. *Gastroenterology*, *159*(4), 1471-1486.e12.  
<https://doi.org/10.1053/j.gastro.2020.06.010>
- Rinella, M. E., & Sookoian, S. (2023). From NAFLD to MASLD: Updated naming and diagnosis criteria for fatty liver disease. *Journal of Lipid Research*, *65*(1), 100485.  
<https://doi.org/10.1016/j.jlr.2023.100485>

- Roy, T. L., Llopis, M., Lepage, P., Bruneau, A., Rabot, S., Bevilacqua, C., Martin, P., Philippe, C., Walker, F., Bado, A., Perlemuter, G., Cassard-Doulcier, A.-M., & Gérard, P. (2013). Intestinal microbiota determines development of non-alcoholic fatty liver disease in mice. *Gut*, *62*(12), 1787–1794.  
<https://doi.org/10.1136/gutjnl-2012-303816>
- Shang, J., Chen, L., Xiao, F., Sun, H., Ding, H., & Xiao, H. (2008). Resveratrol improves non-alcoholic fatty liver disease by activating AMP-activated protein kinase. *Acta Pharmacologica Sinica*, *29*(6), 698–706. <https://doi.org/10.1111/j.1745-7254.2008.00807.x>
- Ströbel, S., Kostadinova, R., Fiaschetti-Egli, K., Rupp, J., Bieri, M., Pawlowska, A., Busler, D., Hofstetter, T., Sanchez, K., Grepper, S., & Thoma, E. (2021). A 3D primary human cell-based in vitro model of non-alcoholic steatohepatitis for efficacy testing of clinical drug candidates. *Scientific Reports*, *11*(1), 22765.  
<https://doi.org/10.1038/s41598-021-01951-7>
- Verma, S., Jensen, D., Hart, J., & Mohanty, S. R. (2013). Predictive value of ALT levels for non-alcoholic steatohepatitis (NASH) and advanced fibrosis in non-alcoholic fatty liver disease (NAFLD). *Liver International*, *33*(9), 1398–1405.  
<https://doi.org/10.1111/liv.12226>
- Vilar-Gomez, E., Martinez-Perez, Y., Calzadilla-Bertot, L., Torres-Gonzalez, A., Gra-Oramas, B., Gonzalez-Fabian, L., Friedman, S. L., Diago, M., & Romero-Gomez, M. (2015). Weight Loss Through Lifestyle Modification Significantly Reduces

- Features of Nonalcoholic Steatohepatitis. *Gastroenterology*, *149*(2), 367-378.e5.  
<https://doi.org/10.1053/j.gastro.2015.04.005>
- Wang, Y., Wang, H., Deng, P., Tao, T., Liu, H., Wu, S., Chen, W., & Qin, J. (2020). Modeling Human Nonalcoholic Fatty Liver Disease (NAFLD) with an Organoids-on-a-Chip System. *ACS Biomaterials Science & Engineering*, *6*(10), 5734–5743. <https://doi.org/10.1021/acsbomaterials.0c00682>
- Wong, V. W.-S., Ekstedt, M., Wong, G. L.-H., & Hagström, H. (2023). Changing epidemiology, global trends and implications for outcomes of NAFLD. *Journal of Hepatology*, *79*(3), 842–852. <https://doi.org/10.1016/j.jhep.2023.04.036>
- Yan, Y., Hou, D., Zhao, X., Liu, J., Cheng, H., Wang, Y., & Mi, J. (2017). Childhood Adiposity and Nonalcoholic Fatty Liver Disease in Adulthood. *Pediatrics*, *139*(4), e20162738. <https://doi.org/10.1542/peds.2016-2738>
- Zeybel, M., Hardy, T., Robinson, S. M., Fox, C., Anstee, Q. M., Ness, T., Masson, S., Mathers, J. C., French, J., White, S., & Mann, J. (2015). Differential DNA methylation of genes involved in fibrosis progression in non-alcoholic fatty liver disease and alcoholic liver disease. *Clinical Epigenetics*, *7*(1), 25.  
<https://doi.org/10.1186/s13148-015-0056-6>
- Zhu, L., Baker, S. S., Gill, C., Liu, W., Alkhouri, R., Baker, R. D., & Gill, S. R. (2013). Characterization of gut microbiomes in nonalcoholic steatohepatitis (NASH) patients: A connection between endogenous alcohol and NASH. *Hepatology (Baltimore, Md.)*, *57*(2), 601–609. <https://doi.org/10.1002/hep.26093>

**VITA**

